





Research Article

Late glacial–Younger Dryas climate in interior Alaska as inferred from the isotope values of land snail shells

Catherine B. Nield¹ , Yurena Yanes¹, Joshua D. Reuther^{2,3} , Daniel R. Muhs⁴, Jeffrey S. Pigati⁴ , Joshua H. Miller¹  and Patrick S. Druckenmiller^{2,5}

¹Department of Geology, University of Cincinnati, Cincinnati, OH 45221, USA; ²University of Alaska Museum, Fairbanks, AK 99775, USA; ³Department of Anthropology, University of Alaska Fairbanks, Fairbanks, AK 99775, USA; ⁴U.S. Geological Survey, USGS, Denver Federal Center, Box 25046, MS 980, Denver, CO 80225, USA and ⁵Department of Geosciences, University of Alaska Fairbanks, Fairbanks, AK 99775, USA

Abstract

The isotope values of fossil snail shells can be important archives of climate. Here, we present the first carbon ($\delta^{13}\text{C}$) and oxygen ($\delta^{18}\text{O}$) isotope values of snail shells in interior Alaska to explore changes in vegetation and humidity through the late-glacial period. Snail shell $\delta^{13}\text{C}$ values were relatively consistent through the late glacial. However, late-glacial shell $\delta^{13}\text{C}$ values are 2.8‰ higher than those of modern shells. This offset is best explained by the Suess effect and changes in the $\delta^{13}\text{C}$ values of snail diet. Snail shell $\delta^{18}\text{O}$ values varied through the late glacial, which can be partially explained by changes in relative humidity (RH). RH during the snail growing period was modeled based on a published flux balance model. Results suggest a dry period toward the beginning of the Bølling–Allerød (~14 ka) followed by two distinct stages of the Younger Dryas, a wetter stage in the early Younger Dryas from 12.9 to 12.3 ka, and subsequent drier stage in the late Younger Dryas between 12.3 and 11.7 ka. The results show that land snail isotopes in high-latitude regions may be used as a supplementary paleoclimate proxy to help clarify complex climate histories, such as those of interior Alaska during the Younger Dryas.

Keywords: Isotopes, Land snails, Younger Dryas, Relative humidity, High latitudes

(Received 5 May 2023; accepted 31 August 2023)

INTRODUCTION

The late Pleistocene was characterized by dramatic changes in climate. This period covers both glacial (Marine Isotope Stages [MIS] 4 and 2) and interglacial periods (MIS 5 and 3). The late-glacial period (~16–12 ka; ka = thousands of years before present [BP]; 0 years BP = AD 1950) marks the transition from the last glacial episode (115–11.7 ka) to the interglacial Holocene (past 11.7 ka) (Walker et al., 2009). With the onset of the warming Holocene epoch, organisms had to adapt, migrate, or go extinct. The late-glacial transitional period was characterized by cold stadial and warm interstadial phases, as seen in Greenland ice core records (Seierstad et al., 2014). Two well-studied stadial episodes during the late glacial are the so-called Oldest Dryas (16–15 ka) and Younger Dryas (12.9–11.7 ka) (Broecker et al., 2010).

The Younger Dryas (12.9–11.7 ka) was a reversal of a warming period (Bølling–Allerød) (14.7–12.9 ka) and a temporary return to glacial like conditions (Broecker et al., 2010). Climate during the Younger Dryas was complex and varied spatially (Kaufman et al., 2010). Evidence for the Younger Dryas is strongest in the

North Atlantic region but is observable in many areas across the world. Emerging evidence from sediment cores in the North Atlantic, western Europe, east Asia, and western North America suggest the Younger Dryas can be grouped into two distinct stages (Brauer et al., 1999; Bakke et al., 2009; Kaufman et al., 2010; Schlolaut et al., 2017; Pigati and Springer, 2022). The first stage, the early Younger Dryas (~12.9–12.3 ka), is characterized by stable conditions due to a weakened Atlantic Meridional Overturning Circulation (AMOC), and the second stage, the late Younger Dryas (12.3–11.7 ka), is defined by variable conditions as the AMOC began to strengthen (Pigati and Springer, 2022). The AMOC is an important component of the Earth's climate system that transports warm water from the tropics to the North Atlantic Ocean, where it cools and sinks before returning southward. The AMOC helps regulate temperatures and influence weather patterns globally. As noted, at the start of the Younger Dryas, the AMOC weakened, leading to a decrease in the amount of warm water transported to the North Atlantic Ocean. This reduction in the poleward transport of warm ocean water likely played a role in triggering a cold period lasting from 12.9 to 11.7 ka and had significant impacts on global climate and ecosystems (Alley et al., 1993). Understanding the behavior of climatic responses to the AMOC is critical for forecasting future climate changes, as recent observations suggest the AMOC has been gradually weakening over the past several decades (Boers, 2021).

Corresponding author: Catherine B. Nield; Email: nieldce@mail.uc.edu

Cite this article: Nield CB, Yanes Y, Reuther JD, Muhs DR, Pigati JS, Miller JH, Druckenmiller PS (2024). Late glacial–Younger Dryas climate in interior Alaska as inferred from the isotope values of land snail shells. *Quaternary Research* 117, 119–134. <https://doi.org/10.1017/qua.2023.54>

© The Author(s), 2023. Published by Cambridge University Press on behalf of Quaternary Research Center. This is an Open Access article, distributed under the terms of the Creative Commons Attribution licence (<http://creativecommons.org/licenses/by/4.0/>), which permits unrestricted re-use, distribution and reproduction, provided the original article is properly cited.



While the effects of climate change are often manifested globally, polar regions have exhibited greater vulnerability to current rapid global warming (Stewart et al., 2013). Changes in Arctic climate have global repercussions that are forecast to intensify in the future. Alaska specifically is warming three to four times as fast as the rest of the United States (Taylor et al., 2017; Walsh and Brettschneider, 2019). Since the 1950s, Alaska's average annual air temperatures have increased by 1.5°C, and average winter temperatures have increased by 4°C (Walsh and Brettschneider, 2019). Paleoclimate records from climate-sensitive regions are thus critical for developing a better understanding of the biological impacts of climate change at both organismal and ecosystem scales.

Despite the significance of these regions in past and present climate change, oxygen and carbon isotopic paleoclimate records in interior Alaska are rare. A few studies have looked at $\delta^{18}\text{O}$ records of diatom silica from Alaska lake sediments (Hu and Shemesh, 2003; Kaufman et al., 2012). Nevertheless, using other terrestrial climate proxies is essential to deepen our understanding of climate transitions in the past, which also provides clues for future climate change. Here, we investigate the utility of land snails as a new paleoclimate proxy for interior Alaska across a range of sedimentary and archaeological settings, to develop a better understanding of late-glacial climatic conditions in interior Alaska.

Land snails are useful indicators of the environment due to their widespread occurrence and abundance and the persistence of their shells after they die. In North America alone, there are around 1200 species of land snails (Nekola, 2014). While the greatest variety of species is found at tropical latitudes, land snails can be found in all terrestrial environments except extremely dry deserts (e.g., Yanes et al., 2019). Their shells are made of aragonite (CaCO_3) (Balakrishnan and Yapp, 2004) and can commonly be found in Quaternary sediment archives worldwide (Goodfriend, 1992).

Land snail shell $\delta^{13}\text{C}$ has been studied in both natural (Goodfriend and Ellis, 2000; Yanes et al., 2008) and laboratory settings (Stott, 2002; Metref et al., 2003; Zhang et al., 2018). A model developed by Goodfriend and Hood (1983) proposed that land snail carbon is derived from three sources: (1) snail diet, (2) atmospheric CO_2 , and (3) ingested carbonates (including limestone and recycled snail shell). However, recent studies have found that ingested carbonates do not seem to affect the shell $\delta^{13}\text{C}$ of small (<5 mm) *Succineidae* shells (Pigati et al., 2004, 2013). Hence, stable carbon isotope values of land snail shells are most often used to infer the carbon isotope compositions of local vegetation and, where present, calculate the relative proportions of C_3 , C_4 , and CAM plants in a given setting (Goodfriend and Stipp, 1983; Goodfriend, 1990; Yanes et al., 2008, 2009).

While snail shell $\delta^{18}\text{O}$ compositions are most commonly used to reconstruct $\delta^{18}\text{O}$ values from precipitation experienced during a snail's active period (Goodfriend, 1991; Zanchetta et al., 2005; Yanes et al., 2011), Balakrishnan and Yapp (2004) showed that the oxygen isotope composition of land snail shells is also controlled by relative humidity (RH) and temperature, as well as by the $\delta^{18}\text{O}$ composition of local precipitation and water vapor. Because land snails are mainly active during or after rain events (Ward and Slotow, 1992), most of the water absorbed by a snail and in a snail's body fluid is derived from rainwater (Riddle, 1983). The flux balance mixing model by Balakrishnan and Yapp (2004) demonstrates that shells are precipitated in oxygen isotopic equilibrium with the snail body fluid. While snails are forming their shells, the body fluid and shell experience ^{18}O enrichment due to evaporation, by about 2‰ on average,

compared with that of the source precipitation (Lécolle, 1985; Goodfriend, 1992; Balakrishnan and Yapp, 2004).

Here, we report the first oxygen and carbon isotope values of fossil land snail shells from interior Alaska, retrieved from an array of Quaternary depositional settings. The shells are constrained chronologically by stratigraphy and/or radiocarbon dating. The stable isotope results are interpreted in the context of a published flux balance mixing model and compared with other published climate proxy records to elucidate the complex late-glacial climate history of interior Alaska.

BACKGROUND

Modern climate and environment in interior Alaska

Crucial to interpretations of stable isotopic compositions of fossil land snails is an understanding of how modern snails are conditioned to today's climate. Nield et al. (2022) found that the $\delta^{18}\text{O}$ values of modern *Succinea strigata* and *Euconulus fulvus* shells are correlated with temperature and precipitation $\delta^{18}\text{O}$ between April and October; they referred to this as the "extended growing season." Interior Alaska can be described as having a continental climate that is largely driven by the distance to oceanic moisture and the precipitation shadows formed by both the Brooks Range to the north and the Alaska Range to the south (Pewe, 1975). This climatic setting supports a boreal forest biome in most of interior Alaska. Typical trees in the Alaskan boreal forest include white spruce (*Picea glauca*), black spruce (*Picea mariana*), larch (*Larix*), balsam poplar (*Populus balsamifera*), aspen (*Populus tremuloides*), Alaska birch (*Betula neoalaskana*), willow (*Salix polaris*), and alder (*Alnus*) (Viereck and Little, 1994). Interior Alaska receives, on average, 305 mm of rain per year and 1550 mm of snow per year (statesummaries.sncics.org, accessed January 2023). Precipitation in interior Alaska is derived mainly from North Pacific Ocean moisture (Abbott et al., 2000). Based on modeled outputs (IAEA/WMO, 2015; Bowen et al., 2005), the average $\delta^{18}\text{O}$ value for precipitation during the snail extended growing season is -17.1‰ (Bowen, 2020). Average extended summer RH is 60% (www.ncdc.noaa.gov, accessed August 2020). Average high and low temperatures during the extended growing season are 14°C and 2°C, respectively (www.usclimatedata.org, accessed August 2020).

Late-glacial climate and environment in interior Alaska

Based on interpretations of lake and peat pollen records throughout Alaska, climate conditions during the Younger Dryas were spatially complex (Kokorowski et al., 2008). Nevertheless, despite high spatial variability, these proxy records consistently indicate that Younger Dryas temperature changes in interior Alaska were muted compared with the North Atlantic region (Graf and Bigelow, 2011). Most records from interior Alaska do not record a sharp temperature reversal at the onset of the Younger Dryas, unlike those that can be seen in Greenland ice core records (Alley et al., 1993). Pollen records from Windmill Lake (interior Alaska) do not show evidence for RH changes during the Younger Dryas (Bigelow and Edwards, 2001). In contrast, these records indicate cool and dry conditions during the Bølling-Allerød that were replaced by high lake levels at the onset of the Holocene (Bigelow and Edwards, 2001). Similarly, using branched glycerol dialkyl glycerol tetraethers (brGDGT) from loess-paleosol sequences as a temperature proxy, Kielhofer and

colleagues (2023) found no dramatic temperature change at the onset or during the Younger Dryas.

Shifts in microfloral fossils indicate mild changes in climate during this time as well. During the late glacial (~16–11.7 ka), interior Alaska was characterized by herb-rich tundra vegetation (Bigelow and Powers, 2001; Anderson, 2003). In the Tanana River valley, vegetation shifted from herb tundra to shrub tundra dominated by birch around ~14 ka. This switch from herb to birch tundra points to a warming air temperature and increased precipitation at ~14 ka (Anderson, 2003). Land snails were collected from deposits dated to these time periods in order to test these hypotheses about paleoclimate shifts in interior Alaska.

MATERIALS AND METHODS

Modern land snail assemblages

Modern snails were collected live from seven locations in the boreal forest in interior Alaska for two summer seasons, 2015 and 2022 (Fig. 1). Sampling took place for 1 hour at each field location where all living and recently dead snails found were collected within a 20 m radius. Field locations were chosen based primarily on their accessibility; however, all localities are representative of a modern, undisturbed boreal forest. Sampled modern sites in interior Alaska contained up to five land snail species, including *S. strigata*, *E. fulvus*, *Columella simplex*, *Discus whitneyi*, and *Punctum* sp. However, in this study, isotopic analyses were conducted on the most abundant and widespread genus, *Succinea*, to taxonomically standardize our comparisons through time, thus removing isotopic variability associated with different species' vital rates, body sizes, or ecologies (Yanes et al., 2017). The family Succineidae exhibits a broad spatial distribution, with shells present on almost every continent. Succineids are associated with highly humid swamp and flooded areas and typically live for 1–2 yr (Oerstan, 2010). However, recent field analysis has observed succineids in drier areas as well, and they are frequently recovered from Quaternary loess deposits of North America (Pigati et al., 2010, 2013) and Europe (Moine et al., 2005).

Late-glacial snail assemblages

Six sites dating to the late-glacial period containing pristine fossil snail shells were investigated in this study (Figs. 1 and 2). In sharp contrast to modern assemblages, most late glacial-age sites contained only one genus, *Succinea* (Fig. 3). However, the permafrost tunnel site, described below, contained three genera, including *Succinea*, *Columella*, and *Euconulus*. A total of 121 fossil shells were selected for isotope analysis (Table 1). Snail shells collected from all paleontological sites were handpicked and sieved from bulk sediment.

The Cold Regions Research and Engineering Laboratory (CRREL) permafrost tunnel is a human-made tunnel that penetrates sediments of the Goldstream Creek valley near Fairbanks, Alaska (Figs. 1 and 2). The tunnel exposes fossiliferous reworked loess and alluvial sediments. Much has been published on the permafrost stratigraphy, ice formations, and preserved fossils at this site (e.g., Hamilton et al., 1988; Shur et al., 2004; Kanevskiy et al., 2022). However, analyses have yet to be done on the snails in these deposits. Ages for loess within the tunnel range from ~34 to ~9.5 ka (Hamilton et al., 1988). Snails from the tunnel were collected via handpicking or sieving of bulk sediment. Snails were found in two areas within the tunnel, referred to as facies

A and facies B. Facies B is an organic-rich area on the ceiling of the tunnel located at the top of the winze (for more details, see Hamilton et al., 1988). Facies A is poorly sorted loess to large cobble-sized sediment located on the floor of the tunnel 12–13 m from the tunnel entrance. The tunnel was constrained chronologically for each facies by several radiocarbon ages from shells and plant remains (Table 2). The isotopic values of 13 *Succinea* shells were determined from these deposits, dating to ~14 ka.

Snails were also collected from last glacial loess road outcrops along the Dalton Highway. Snails were found in two locations sampled by Muhs et al. (2018), at milepost 45.9 (AK-650A) and milepost 54.7 (AK-855). While Quaternary loess is common throughout Alaska, loess dating to the last glacial period in Alaska is rare (Muhs et al., 2018). The Dalton Highway sites present unusual occurrences of last glacial loess deposits dating from 19 to 12 ka in the Yukon-Tanana Upland (Figs. 1 and 2). At these sites, *Succinea* shells were found in the upper parts of loess sections. Calibrated radiocarbon ages of snails span an interval between ~13.4 and ~12.7 ka (Muhs et al., 2018). At these sites, 36 *Succinea* shells were selected for isotopic analysis.

To complement sampling at paleontological sites, we also retrieved land snail shells from four Alaskan archaeological sites: Mead, Upward Sun River (USRS), North Gerstle, and Bachner (Figs. 1 and 2). Each site has loess deposits that are greater than 1 m in thickness. The Mead archaeological site is located along Shaw Creek Bluff near Delta Junction (Dilley, 1998) and is interpreted as a human base camp (Potter et al., 2013). *Succinea* shells were found in a trench away from the main archaeological excavation in stratigraphic zones dated to ~12.6 to 11.8 ka (Kielhofer et al., 2020). Here, 10 *Succinea* shells were analyzed for isotopes. The Upward Sun River site is located on a loess-covered dune near the Tanana River valley (Reuther, 2013). Cultural remains come from repeated occupations of the dune dating back to 13.3 ka and include a late-glacial residential structure and the cremated and buried remains of a child (Potter et al., 2011, 2014). 20 *Succinea* shells were analyzed for isotopes from horizons dated to ~13.1–12.6 ka. The North Gerstle site is also in the Tanana River valley on a bluff overlooking the Tanana River. *Succinea* shells were collected from horizons dated to 12.9–12.8 ka (Vanderhoek et al., 1997). Here, 18 *Succinea* shells were selected for analyses. The Bachner site overlooks Quartz Lake and is adjacent to Shaw Creek Flats, also within the Tanana River valley, within 10 km of the Mead and North Gerstle sites (Reuther, 2013). *Succinea* shells were found at layers dated to ~12.8–11.9 ka, and 25 *Succinea* shells were analyzed for isotopes.

Radiocarbon dating

For this study, fossil *Succinea* shells were either radiocarbon dated directly or collected from a horizon where the chronology is well constrained by radiocarbon dating of other shells, plant macrofossils, wood, or charcoal. Three snail samples collected from the CRREL permafrost tunnel were selected for paired graphite-target and carbonate-target radiocarbon dating analysis (Bright et al., 2021; Fig. 4). Historically, land snail shells have been avoided for radiocarbon dating because of the potential incorporation of ^{14}C from limestone during shell formation (Pigati et al., 2004). However, several genera of small gastropods, including Succineidae, have been shown to provide reliable radiocarbon ages (Pigati et al., 2004). To further verify the age of snail shells from the permafrost tunnel, two plant remains samples taken

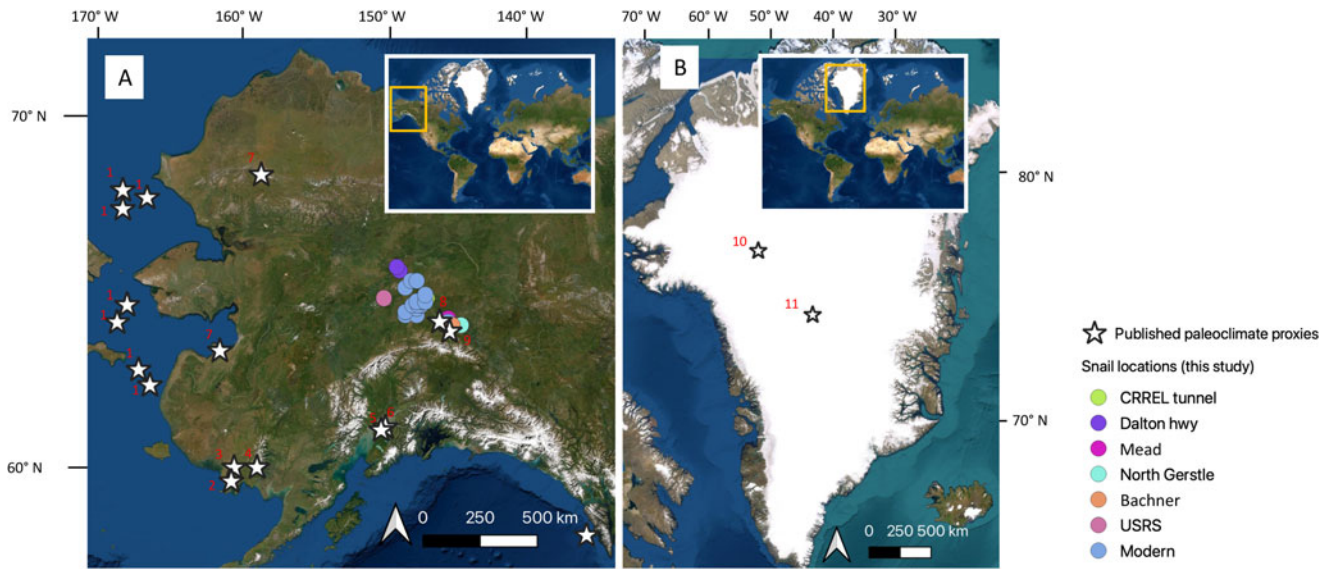


Figure 1. (A) Quaternary depositional settings (circles) where fossil shells and modern snails were sampled (this study). Studied sites include permafrost soils (Cold Regions Research and Engineering Laboratory [CRREL] tunnel), loess deposits (Dalton highway), and archaeological sites (Mead, Bachner, North Gerstle, and Upward Sun River [USRS]). Published paleoclimate proxy sites (white stars), including marine cores, lake cores, and paleosols (see text). (B) Map of Greenland showing locations of two previously published paleoclimate proxies from ice cores; North Greenland Ice Core Project (NGRIP; north location) and North Greenland Eemian Ice Drilling (NEEM; south location). Locations of paleoclimate proxies in the published literature: (1) Grebmeier *et al.*, 1990; (2) Hu *et al.*, 2002; (3) Hu *et al.*, 2006; (4) Kaufman *et al.*, 2012; (5) Kaufman *et al.*, 2009; (6) Jones *et al.*, 2009; (7) Kurek *et al.*, 2009; (8) Abbott *et al.*, 2000; (9) Kielhofer *et al.*, 2023; (10) NGRIP Members, 2004; (11) Masson-Delmotte *et al.*, 2015.

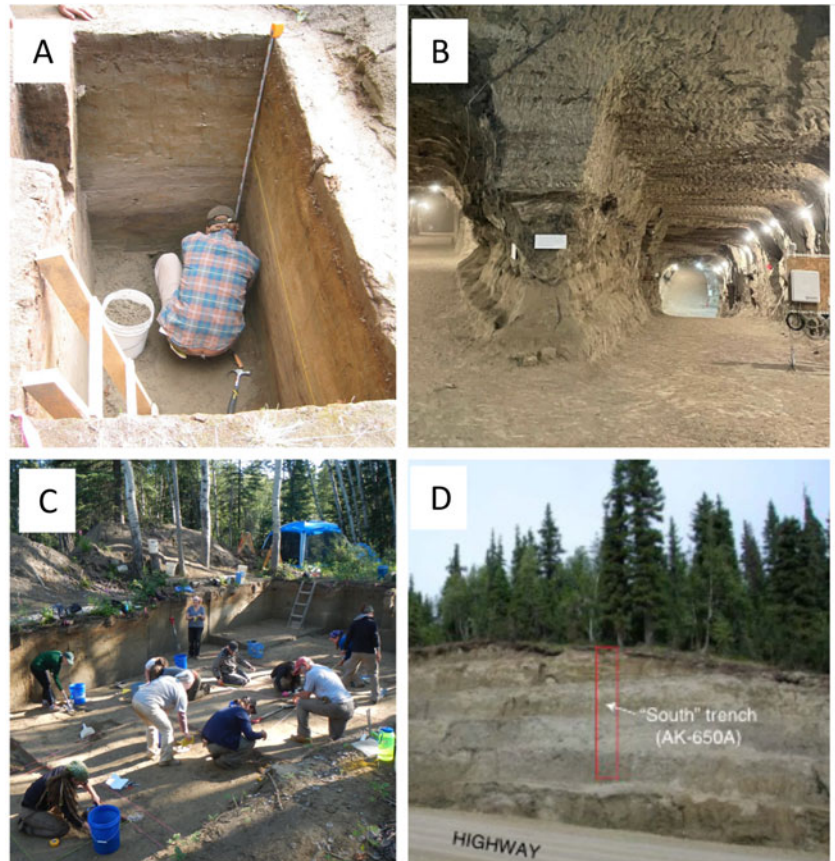


Figure 2. Photographs where late-glacial snail shells were collected. (A) Mead archaeological site. (B) Cold Regions Research and Engineering Laboratory (CRREL) permafrost research tunnel. (C) Upward Sun River archaeological site. (D) Yukon-Tanana Upland loess deposits at Dalton highway (adapted from Muhs *et al.*, 2018).

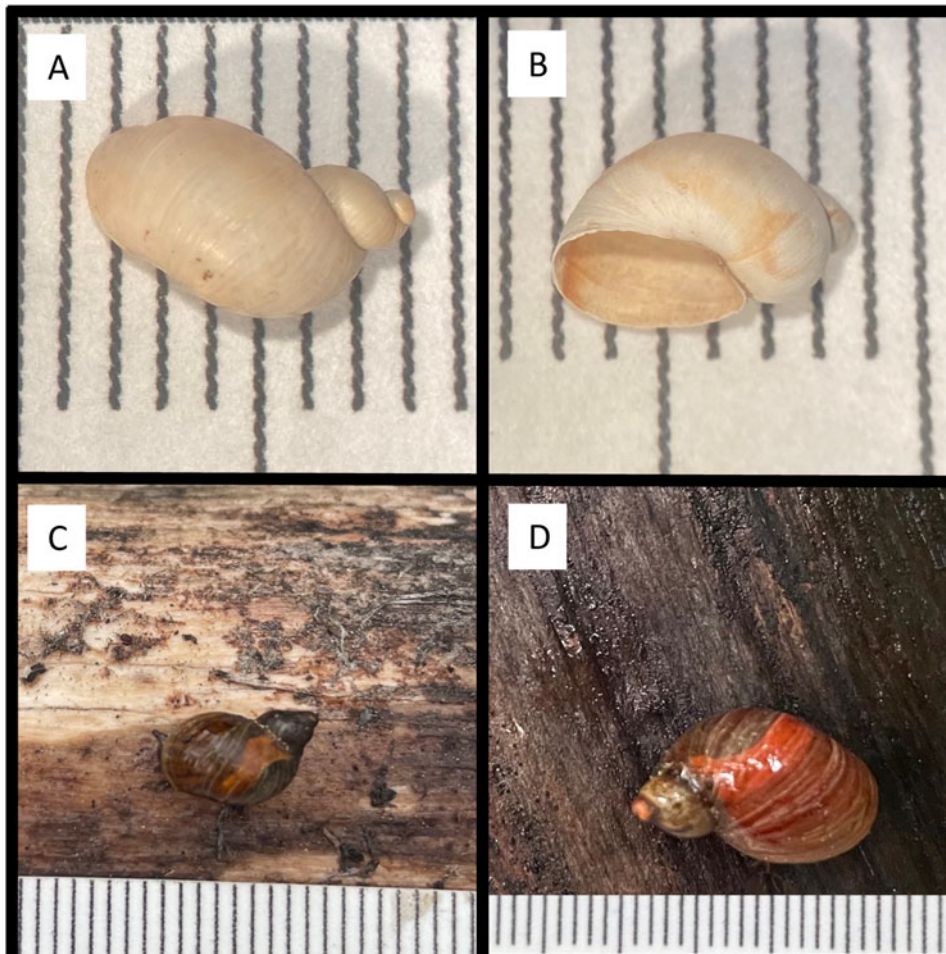


Figure 3. Photographs of modern and fossil *Succinea* specimens. Pictures depict (A and B) late-glacial (~14,000 cal yr BP) specimens retrieved from the Cold Regions Research and Engineering Laboratory (CRREL) permafrost tunnel and (C and D) living *Succinea* specimens found in the forest near Fairbanks, Alaska. Scales are in millimeters.

from the same horizon as the snail assemblage were radiocarbon dated and yielded results similar to those of the shells (Table 2).

Late-glacial *Succinea* shells from loess deposits and archaeological sites have been radiocarbon dated in prior work (Potter et al., 2011, 2013; Reuther, 2013; Muhs et al., 2018; Kielhofer et al., 2020). Sections at the Bachner and North Gerstle site were previously dated using charcoal and collagen from animal bones (Reuther, 2013). For the present study, shells from these deposits were radiocarbon dated (Table 2) at the Center for Applied Isotope Studies at the University of Georgia, following procedures outlined in their laboratory protocols (<https://cais.uga.edu/service/radiocarbon-dating-by-ams>). Shell and plant remains from the CRREL permafrost tunnel were radiocarbon dated at the W.M. Keck Carbon Cycle Accelerator Mass Spectrometry Laboratory at the University of California–Irvine following the procedures outlined in their laboratory protocols (<https://www.ess.uci.edu/group/ams/protocols>). Shells were dated using the carbonate-target and graphite-target radiocarbon methods, and detailed methodology for both dating methods can be found in Bright et al. (2021). The resultant radiocarbon ages were all calibrated to calendar years using the IntCal20 data set and CALIB 8.20 (Reimer et al., 2020).

Stable isotope analyses

In total, 174 individual shells were selected for isotope analysis by choosing the cleanest and best-preserved shells. Shells were mechanically cleaned with deionized water to remove any remaining debris and air-dried before laboratory analysis. Land snail shells were analyzed at the University of Florida using a Finnigan-MAT 252 Isotope Ratio Mass Spectrometer coupled with a Kiel III automated carbonate preparation device. Additional details of the methodology can be found in Nield et al. (2022). Analytical precision was better than $\pm 0.1\%$, as shown by repeated measurements of samples and standards. Results were calibrated against the international standards NBS-18 and NBS-19.

Statistical analyses

All statistical analyses were done using R v. 2.5.1 software (R Core Team, 2023). All data were treated as nonnormally distributed. The Kruskal-Wallis test was used to determine whether the multiple groups exhibited statistically equivalent median values. The Mann-Whitney test was used when comparing the median value between two groups only. Statistical significance was accepted when the *P* value was less than 0.05. Pearson correlation analysis was conducted to assess the significance of monotonic

Table 1. Carbon and oxygen isotope compositions of modern and fossil *Succinea* shells from central Alaska with median calibrated ages (BP).^a

Taxa	Location	$\delta^{18}\text{O}$ (PDB)	$\delta^{13}\text{C}$ (PDB)	Age (Cal BP)	±	Taxa	Location	$\delta^{18}\text{O}$ (PDB)	$\delta^{13}\text{C}$ (PDB)	Age (Cal BP)	±
<i>Succinea</i>	Fairbanks Forest	-9.1	-10.9	Modern	-	<i>Succinea</i>	Dalton hwy	-11.5	-7.9	12,920	50
<i>Succinea</i>	Fairbanks Forest	-9.5	-10.5	Modern	-	<i>Succinea</i>	Dalton hwy	-12.2	-6.3	12,920	50
<i>Succinea</i>	Fairbanks Forest	-12.8	-10.2	Modern	-	<i>Succinea</i>	Dalton hwy	-11.6	-7.5	12,940	80
<i>Succinea</i>	Fairbanks Forest	-11.3	-11.0	Modern	-	<i>Succinea</i>	Dalton hwy	-12.5	-7.4	12,940	80
<i>Succinea</i>	Fairbanks Forest	-10.2	-11.7	Modern	-	<i>Succinea</i>	Dalton hwy	-11.7	-7.1	12,940	80
<i>Succinea</i>	Fairbanks Forest	-10.9	-11.3	Modern	-	<i>Succinea</i>	Dalton hwy	-11.1	-6.7	12,940	80
<i>Succinea</i>	Fairbanks Forest	-10.0	-7.9	Modern	-	<i>Succinea</i>	Dalton hwy	-11.5	-6.9	13,010	80
<i>Succinea</i>	Fairbanks Forest	-10.8	-10.4	Modern	-	<i>Succinea</i>	Dalton hwy	-11.8	-6.6	13,010	80
<i>Succinea</i>	Fairbanks Forest	-9.6	-11.4	Modern	-	<i>Succinea</i>	Dalton hwy	-11.5	-7.9	13,010	80
<i>Succinea</i>	Fairbanks Forest	-10.8	-10.7	Modern	-	<i>Succinea</i>	Dalton hwy	-12.3	-6.5	13,010	80
<i>Succinea</i>	Fairbanks Forest	-11.8	-11.8	Modern	-	<i>Succinea</i>	Dalton hwy	-11.9	-7.2	13,010	100
<i>Succinea</i>	Fairbanks Forest	-11.0	-10.0	Modern	-	<i>Succinea</i>	Dalton hwy	-12.8	-7.9	13,010	100
<i>Succinea</i>	Fairbanks Forest	-11.1	-11.4	Modern	-	<i>Succinea</i>	Dalton hwy	-12.7	-7.4	13,010	100
<i>Succinea</i>	Fairbanks Forest	-11.5	-12.7	Modern	-	<i>Succinea</i>	Dalton hwy	-12	-8.1	13,040	90
<i>Succinea</i>	Fairbanks Forest	-10.3	-10.9	Modern	-	<i>Succinea</i>	Dalton hwy	-12.7	-7.8	13,040	90
<i>Succinea</i>	Fairbanks Forest	-10.4	-10.3	Modern	-	<i>Succinea</i>	Dalton hwy	-11.9	-7.8	13,040	90
<i>Succinea</i>	Fairbanks Forest	-11.3	-10.5	Modern	-	<i>Succinea</i>	Dalton hwy	-11.4	-6.7	13,040	90
<i>Succinea</i>	Fairbanks Forest	-10.8	-10.4	Modern	-	<i>Succinea</i>	Dalton hwy	-12.3	-6.3	13,170	90
<i>Succinea</i>	Fairbanks Forest	-10.9	-10.2	Modern	-	<i>Succinea</i>	Dalton hwy	-13.7	-7.9	13,170	90
<i>Succinea</i>	Fairbanks Forest	-10.7	-10.4	Modern	-	<i>Succinea</i>	Dalton hwy	-11.8	-6.3	13,170	90
<i>Succinea</i>	Fairbanks Forest	-10.7	-10.8	Modern	-	<i>Succinea</i>	Dalton hwy	-12	-6.4	13,170	90
<i>Succinea</i>	Fairbanks Forest	-10.8	-10.2	Modern	-	<i>Succinea</i>	Dalton hwy	-12.9	-7.9	13,410	120
<i>Succinea</i>	Fairbanks Forest	-10.8	-9.9	Modern	-	<i>Succinea</i>	Dalton hwy	-11.9	-7.1	13,410	120
<i>Succinea</i>	Fairbanks Forest	-10.4	-10.8	Modern	-	<i>Succinea</i>	Dalton hwy	-12	-7	13,410	120
<i>Succinea</i>	Fairbanks Forest	-10.8	-10.4	Modern	-	<i>Succinea</i>	Dalton hwy	-11.4	-6.7	13,410	120
<i>Succinea</i>	Fairbanks Forest	-10.9	-10.8	Modern	-	<i>Succinea</i>	CRREL tunnel	-10.5	-9.5	14,060	35
<i>Succinea</i>	Fairbanks Forest	-11.1	-11.0	Modern	-	<i>Succinea</i>	CRREL tunnel	-9.1	-6.3	14,060	35
<i>Succinea</i>	Fairbanks Forest	-10.8	-10.2	Modern	-	<i>Succinea</i>	CRREL tunnel	-9	-5.9	14,060	35
<i>Succinea</i>	Fairbanks Forest	-10.8	-10.7	Modern	-	<i>Succinea</i>	CRREL tunnel	-10.6	-6	14,060	35
<i>Succinea</i>	Fairbanks Forest	-10.3	-10.0	Modern	-	<i>Succinea</i>	CRREL tunnel	-9.2	-6.6	14,060	35
<i>Succinea</i>	Fairbanks Forest	-11.0	-10.1	Modern	-	<i>Succinea</i>	CRREL tunnel	-11.9	-8.2	14,060	35
<i>Succinea</i>	Fairbanks Forest	-11.3	-9.8	Modern	-	<i>Succinea</i>	CRREL tunnel	-10.6	-7.2	14,060	35
<i>Succinea</i>	Fairbanks Forest	-10.6	-10.4	Modern	-	<i>Succinea</i>	CRREL tunnel	-8.6	-7.3	14,060	35
<i>Succinea</i>	Fairbanks Forest	-11.0	-10.3	Modern	-	<i>Succinea</i>	CRREL tunnel	-11.2	-7.6	14,060	35
<i>Succinea</i>	Fairbanks Forest	-10.5	-11.1	Modern	-	<i>Succinea</i>	CRREL tunnel	-10.8	-7.5	14,060	35
<i>Succinea</i>	Fairbanks Forest	-11.3	-9.7	Modern	-	<i>Succinea</i>	CRREL tunnel	-11.9	-7.5	14,060	35
<i>Succinea</i>	Fairbanks Forest	-10.9	-10.8	Modern	-	<i>Succinea</i>	CRREL tunnel	-8.3	-7.7	14,060	35
<i>Succinea</i>	Fairbanks Forest	-10.8	-10.4	Modern	-	<i>Succinea</i>	CRREL tunnel	-12.2	-9.9	14,060	35
<i>Succinea</i>	Fairbanks Forest	-10.8	-10.6	Modern	-	<i>Succinea</i>	The Bachner	-11.53	-7.51	11,870	35
<i>Succinea</i>	Mead	-10.9	-8.4	11,800	30	<i>Succinea</i>	The Bachner	-11.32	-7.94	11.87	35
						<i>Succinea</i>	The Bachner	-12.09	-7.6	11.87	35
<i>Succinea</i>	Mead	-12.0	-8.8	11,800	30	<i>Succinea</i>	The Bachner	-11.73	-7.66	11.87	35

(Continued)

Table 1. (Continued.)

Taxa	Location	$\delta^{18}\text{O}$ (PDB)	$\delta^{13}\text{C}$ (PDB)	Age (Cal BP)	\pm	Taxa	Location	$\delta^{18}\text{O}$ (PDB)	$\delta^{13}\text{C}$ (PDB)	Age (Cal BP)	\pm
<i>Succinea</i>	Mead	-11.5	-8.4	11,800	30	<i>Succinea</i>	The Bachner	-11.79	-8.24	11,870	35
<i>Succinea</i>	Mead	-10.9	-9.3	11,800	30	<i>Succinea</i>	The Bachner	-11.27	-8.2	12,400	35
<i>Succinea</i>	Mead	-10.4	-8.7	12,170	87	<i>Succinea</i>	The Bachner	-12.76	-7.59	12,400	35
<i>Succinea</i>	Mead	-11.7	-9.3	12,170	87	<i>Succinea</i>	The Bachner	-11.55	-7.79	12,400	35
<i>Succinea</i>	Mead	-11.6	-8.7	12,560	190	<i>Succinea</i>	The Bachner	-12.08	-7.45	12,400	35
<i>Succinea</i>	Mead	-11.3	-9.3	12,560	190	<i>Succinea</i>	The Bachner	-11.21	-6.65	12,400	35
<i>Succinea</i>	Mead	-9.6	-8.6	12,560	190	<i>Succinea</i>	The Bachner	-11.58	-7.63	12,400	35
<i>Succinea</i>	Mead	-10.4	-8.4	12,560	190	<i>Succinea</i>	The Bachner	-12.04	-7.38	12,400	35
<i>Succinea</i>	Upward sun river	-13.0	-8.4	12,570	67	<i>Succinea</i>	The Bachner	-11.31	-6.65	12,400	35
<i>Succinea</i>	Upward sun river	-13.1	-7.8	12,570	67	<i>Succinea</i>	The Bachner	-12.05	-6.6	12,400	35
<i>Succinea</i>	Upward sun river	-12.7	-7.8	12,570	67	<i>Succinea</i>	The Bachner	-12.29	-6.96	12,400	35
<i>Succinea</i>	Upward sun river	-12.6	-7.7	12,570	67	<i>Succinea</i>	The Bachner	-11.93	-7.7	12,800	35
<i>Succinea</i>	Upward sun river	-12.6	-8.7	12,570	67	<i>Succinea</i>	The Bachner	-10.28	-8.3	12,800	35
<i>Succinea</i>	Upward sun river	-12.2	-8.1	12,600	67	<i>Succinea</i>	The Bachner	-11.45	-7.59	12,800	35
<i>Succinea</i>	Upward sun river	-11.5	-8.6	12,600	67	<i>Succinea</i>	The Bachner	-10.1	-7.61	12,800	35
<i>Succinea</i>	Upward sun river	-12.1	-8.3	12,600	67	<i>Succinea</i>	The Bachner	-11.08	-7.63	12,800	35
<i>Succinea</i>	Upward sun river	-11.9	-8.8	12,700	60	<i>Succinea</i>	The Bachner	-12.25	-8.39	12,620	35
<i>Succinea</i>	Upward sun river	-11.6	-9.1	12,700	60	<i>Succinea</i>	The Bachner	-11.64	-8.64	12,620	35
<i>Succinea</i>	Upward sun river	-12.3	-9.0	12,700	60	<i>Succinea</i>	The Bachner	-12.08	-8.78	12,620	35
<i>Succinea</i>	Upward sun river	-11.5	-9.3	12,700	60	<i>Succinea</i>	The Bachner	-11.63	-8.55	12,620	35
<i>Succinea</i>	Upward sun river	-10.8	-7.5	12,800	60	<i>Succinea</i>	The Bachner	-11.74	-8.77	12,620	35
<i>Succinea</i>	Upward sun river	-10.4	-8.1	12,800	60	<i>Succinea</i>	North Gerstle	-13.19	-8.08	12,790	30
<i>Succinea</i>	Upward sun river	-11.8	-8.9	12,800	60	<i>Succinea</i>	North Gerstle	-11.96	-7.61	12,790	30
<i>Succinea</i>	Upward sun river	-11.9	-8.7	12,800	60	<i>Succinea</i>	North Gerstle	-12.37	-8.14	12,790	30
<i>Succinea</i>	Upward sun river	-11.2	-7.0	13,130	60	<i>Succinea</i>	North Gerstle	-11.95	-7.37	12,790	30
<i>Succinea</i>	Upward sun river	-11.8	-9.3	13,130	60	<i>Succinea</i>	North Gerstle	-12.93	-7.56	12,790	30
<i>Succinea</i>	Upward sun river	-12.1	-8.6	13,130	60	<i>Succinea</i>	North Gerstle	-12.29	-7.61	12,790	30
<i>Succinea</i>	Upward sun river	-11.3	-7.5	13,130	60	<i>Succinea</i>	North Gerstle	-12.4	-8.05	12,790	30
<i>Succinea</i>	Dalton hwy	-12.1	-7.7	12,710	130	<i>Succinea</i>	North Gerstle	-13.15	-8.52	12,790	30
<i>Succinea</i>	Dalton hwy	-11.9	-7.3	12,710	100	<i>Succinea</i>	North Gerstle	-12.49	-7.29	12,860	30
<i>Succinea</i>	Dalton hwy	-11.4	-7.5	12,720	60	<i>Succinea</i>	North Gerstle	-11.79	-7.76	12,860	30
<i>Succinea</i>	Dalton hwy	-12.0	-7.1	12,720	60	<i>Succinea</i>	North Gerstle	-13.17	-7.68	12,860	30
<i>Succinea</i>	Dalton hwy	-12.3	-7.1	12,720	60	<i>Succinea</i>	North Gerstle	-12.82	-8.47	12,860	30
<i>Succinea</i>	Dalton hwy	-11.2	-7.6	12,720	130	<i>Succinea</i>	North Gerstle	-12.18	-8.1	12,860	30
<i>Succinea</i>	Dalton hwy	-12.3	-7.3	12,790	120	<i>Succinea</i>	North Gerstle	-13.08	-9.22	12,860	30
<i>Succinea</i>	Dalton hwy	-12.3	-8.1	12,790	120	<i>Succinea</i>	North Gerstle	-13.58	-7.62	12,860	30
<i>Succinea</i>	Dalton hwy	-12.2	-6.5	12,790	120	<i>Succinea</i>	North Gerstle	-11.37	-8.02	12,860	30
<i>Succinea</i>	Dalton hwy	-11.6	-7.2	12,920	30	<i>Succinea</i>	North Gerstle	-12.98	-8.33	12,860	30
<i>Succinea</i>	Dalton hwy	-11.9	-7.4	12,920	50	<i>Succinea</i>	North Gerstle	-13.63	-7.58	12,860	30

^aModern snails were live collected in 2015/2022.

Table 2. Sample identifications, radiocarbon ages, and calibrated ages for *Succinea* shells from the Cold Regions Research and Engineering Laboratory (CRREL) permafrost tunnel, the Bachner, and North Gerstle Point sites, and organic matter in the CRREL tunnel.

Lab ref #	Field ref	Material	Location	Rapid carbonate target		Traditional graphite target		2-sigma calibrated age (Cal yr BP)		
				¹⁴ C age (BP)	±	¹⁴ C age (BP)	±	Minimum	Maximum	Median
251864	BOCa	Plant remains	CRREL tunnel	-	-	11,770	35	13,570	13,760	13,640
251865	BOCb	Plant remains	CRREL tunnel	-	-	12,010	30	13,790	14,040	13,910
251872	AWS	Snail shell	CRREL tunnel	12,300	140	12,160	35	13,970	14,200	14,060
251873	ASF	Snail shell	CRREL tunnel	12,500	130	12,180	35	14,000	14,310	14,100
251874	BWS	Snail shell	CRREL tunnel	11,900	120	12,090	35	13,800	14,080	13,940
UGAMS#61066	1581	Snail shell	Bachner	-	-	10,580	35	12,580	12,720	12,620
UGAMS#61067	1717	Snail shell	Bachner	-	-	10,200	30	11,690	12,060	11,870
UGAMS#60834	XBD163-22-283	Snail shell	North Gerstle Point	-	-	10,860	30	12,730	12,850	12,790
UGAMS#60833	XBD163-22-298	Snail shell	North Gerstle Point	-	-	10,950	30	12,750	13,000	12,860

relationships between two variables. The coefficient of determination (R^2) was used to identify the strength of the model and relationship.

RESULTS

Radiocarbon results

Results from the paired graphite-target and carbonate-target radiocarbon dating analysis (Bright et al., 2021) of shells from the CRREL permafrost tunnel show the two dating methods are not statistically different ($R^2 = 0.98$, $P = 0.7$; Fig. 4, Table 2). Both methods yield equivalent ages, although the graphite-target method (± 35 yr) is more precise than the carbonate-target method (± 140 yr). The carbonate-target method is less expensive and uses a far smaller sample, <1 mg compared with 20+ mg, which makes it an attractive option for land snail shell radiocarbon dating. All analyzed snails from the permafrost tunnel date to ~ 14 ka, in agreement with plant remains samples that were taken

from the same horizon (Table 2). Ages of snail shells from the tunnel range from 14.0 to 13.9 ka, and plant remains ages range from 13.9 to 13.6 ka. Other snails sampled from the same assemblage of the CRREL tunnel are provisionally assumed to be the same age. Additional traditional graphite carbon radiocarbon analysis was performed on shells from the Bachner and North Gerstle sites (Table 2). Snails from Bachner were dated to 12.6 and 11.9 ka, and snails from North Gerstle were dated to 12.9 and 12.8 ka.

Carbon isotopic composition

Carbon isotope analyses were performed on 121 fossil and 53 modern *Succinea* shells, and the results are shown as box plots in 250 yr time bins (Fig. 5). Late-glacial shell $\delta^{13}\text{C}$ values average -7.7‰ and range between -9.9‰ and -5.9‰ across the time intervals (Fig. 5, Table 1). Median $\delta^{13}\text{C}$ values of shells from the early Bølling–Allerød (~ 14 ka), early Younger Dryas (12.9–12.3 ka), and late Younger Dryas time (12.3–11.7 ka) are

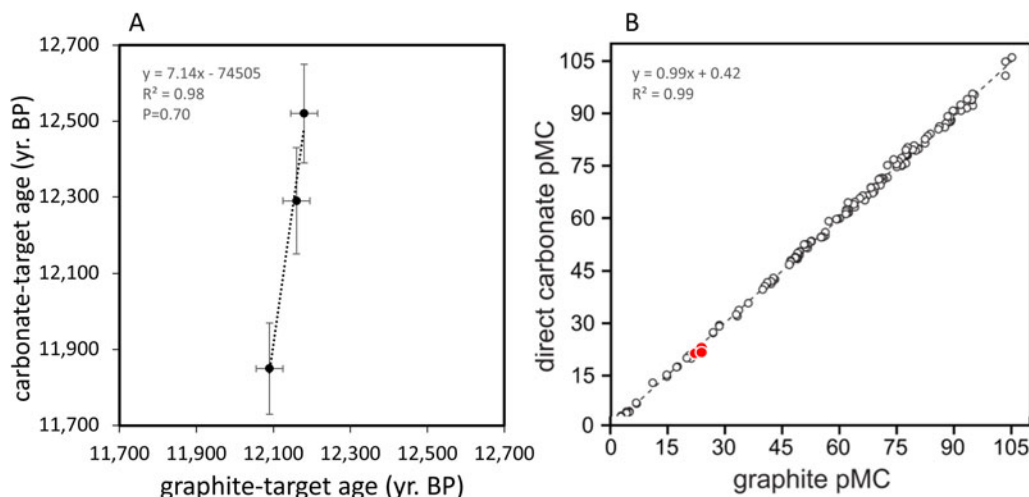


Figure 4. (A) Scatter plot comparing carbonate-target vs. graphite-target radiocarbon-dated *Succinea* shells collected from the Cold Regions Research and Engineering Laboratory (CRREL) permafrost tunnel with error bars for age uncertainty. (B) Data from this study (filled red dots) plotted on figure from Bright et al. (2021). Reduced major axis regression of paired direct carbonate and graphite pMC (percent modern carbon) determinations.

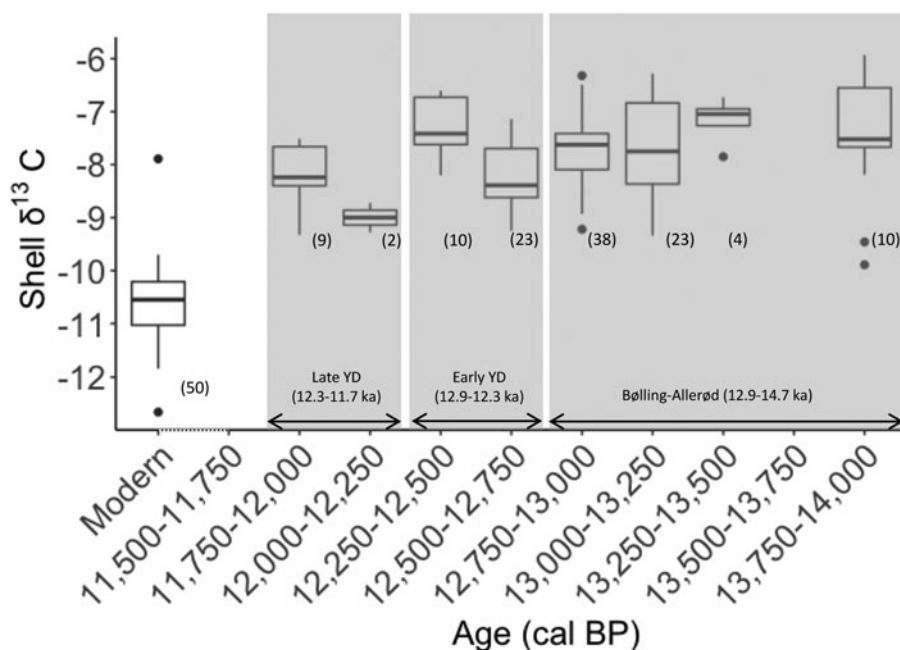


Figure 5. *Succinea* shell $\delta^{13}\text{C}$ values (in PDB, Pee Dee Belemnite) binned into 250 yr time intervals. Box extremes represent lower and upper quartiles. Whiskers depict the range of values. The solid line inside the plot depicts the median $\delta^{13}\text{C}$ value. Number in parentheses is the number of samples. The dots represent outliers that were outside the interquartile range. The three shaded regions mark the Bølling-Allerød (BA) (14.7–12.9 ka), the early Younger Dryas (YD) (12.9–12.3 ka), and the late Younger Dryas (12.3–11.7 ka).

–7.5‰, –7.8‰, and –8.2‰, respectively ($\chi^2 = 9.9792$, $df = 4$, $P = 0.0408$). Median $\delta^{13}\text{C}$ values in late-glacial time bins vary by only 0.7‰. Modern shell $\delta^{13}\text{C}$ values have a median value of –10.9‰, ranging from –12.7‰ to –7.9‰ (Fig. 5). All late-glacial time bins differ significantly from values in modern shells, being on average 2.8‰ higher than modern shells ($W = 6048$, $P < 0.001$).

Oxygen isotopic composition

Oxygen isotope analyses were performed on the same 121 fossil and 53 modern *Succinea* shells as the $\delta^{13}\text{C}$ analysis. The results are illustrated again as box plots and separated into 250 yr bins (Fig. 6). Late-glacial (14–11.5 ka) shell $\delta^{18}\text{O}$ values have a median value of –11.9‰ and range from –13.7‰ to –8.3‰ (Fig. 6B, Table 1). Within this time period, early Bølling-Allerød (~14 ka), early Younger Dryas (12.9–12.3 ka), and late Younger Dryas (12.3–11.7 ka) have median shell $\delta^{18}\text{O}$ values of –10.6‰, –12.1‰, and –11.5‰, respectively, and differ significantly from each other ($\chi^2 = 29.636$, $df = 4$, $P < 0.001$). Modern shell $\delta^{18}\text{O}$ has a median value of –10.8‰ and ranges from –12.8‰ to –8.9‰ (Fig. 6). Late-glacial shell values differ significantly from values in modern shells ($W = 778.5$, $P < 0.001$).

DISCUSSION

Paleo-vegetation inferences

Median modern shell $\delta^{13}\text{C}$ values are 2.8‰ lower than median late-glacial $\delta^{13}\text{C}$ values (Fig. 5). This offset between modern and late-glacial values is likely best explained by shifts in the carbon isotope composition of one or more of the three main components affecting the carbon isotope values of land snail shells: atmospheric carbon, diet, and ingested carbonate (Goodfriend and Ellis, 2002). Of these, changes in atmospheric carbon and diet may be most likely to have produced differences in shell $\delta^{13}\text{C}$. While land snails may consume limestone as a source of calcium to build their shells, and limestone ingestion may be capable

of positively shifting (by several per mil) shell $\delta^{13}\text{C}$ values, recent studies have found that small-bodied Succineidae gastropods may consume only minimal amounts of carbonate sediments (Pigati et al., 2004, 2013).

Since the Industrial Revolution, increased burning of fossil fuels has not only increased CO_2 concentrations but also affected carbon isotopic composition of atmospheric CO_2 . Overall, $\delta^{13}\text{C}$ values of atmospheric CO_2 have become more negative following the Industrial Revolution (Friedli et al., 1986). This decline in atmospheric CO_2 $\delta^{13}\text{C}$ has caused a decline in plant (Dawson et al., 2002), and therefore snail shell, $\delta^{13}\text{C}$ values. This phenomenon is known as the Suess effect (Keeling, 1979). However, the Suess effect can only account for a 1–1.5‰ negative shift in $\delta^{13}\text{C}$ values (Wang et al., 2011). If we apply the correction to the snail shells analyzed here, there would still be an ~1–2‰ decrease in shell $\delta^{13}\text{C}$ composition from the late glacial to today.

The remaining offset between modern and late-glacial shell $\delta^{13}\text{C}$ values is most likely due to differences in the $\delta^{13}\text{C}$ values of the snail diet. Generally, modern tundra, boreal forest, and coastal forest biomes in Alaska are all dominated by C_3 plants (average $\delta^{13}\text{C}$ value of –26‰), which include trees and cool-season grasses and are depleted in ^{13}C compared with C_4 plants (average $\delta^{13}\text{C}$ value of –12‰) (O’Leary, 1988; Muhs et al., 1999, 2000). C_3 and C_4 plants fractionate carbon isotopes in different ways. Soil organic matter in most Alaskan biomes shows $\delta^{13}\text{C}$ values of –25‰ (Muhs et al., 2000). Additionally, none of the $\delta^{13}\text{C}$ analyses from samples taken from the CRREL permafrost tunnel or from nearby Quartz and Goldbottom Creeks are in the range of $\delta^{13}\text{C}$ values of C_4 grasses (Wooller et al., 2018). Laboratory studies have found aragonite carbon of land snail shells to be positively fractionated with respect to the bicarbonate carbon from which it precipitated (Rubinson and Clayton, 1969). This can in part explain why shell $\delta^{13}\text{C}$ values are more positive than consumed plant $\delta^{13}\text{C}$.

C_4 plants are supported by lower atmospheric CO_2 concentrations (Wang et al., 2020). In theory, this could suggest higher concentrations of C_4 plants in Alaska during the last glacial period,

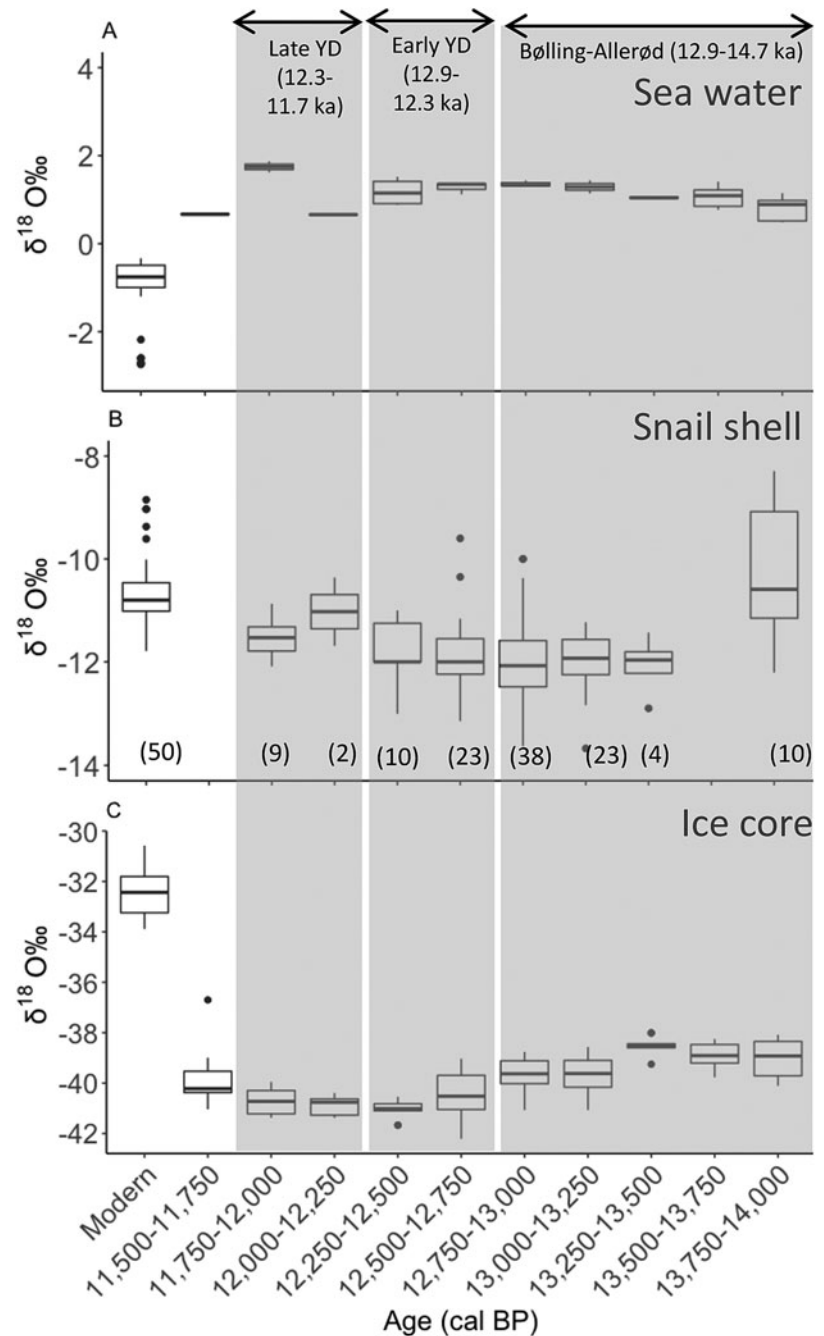


Figure 6. $\delta^{18}\text{O}$ values binned into 250 yr time intervals. The three shaded regions mark the Bølling-Allerød (BA) (14.7–12.9 ka), the early Younger Dryas (YD) (12.9–12.3 ka), and the late Younger Dryas (12.3–11.7 ka). (A) Seawater $\delta^{18}\text{O}$ values (in SMOW) calculated from benthic foraminifera off the coast of Alaska (Grebmeier et al. 1990; Praetorius et al., 2015, 2016); (B) snail shell $\delta^{18}\text{O}$ values (in PDB) of *Succinea* shells from central Alaska; and (C) North Greenland Ice Core Project (NGRIP Members, 2004) and North Greenland Eemian Ice Drilling (NEEM; Masson-Delmotte et al., 2015) Greenland ice core $\delta^{18}\text{O}$ values in SMOW. Box extremes represent lower and upper quartiles. Whiskers depict the range of values. The solid line inside the plot depicts the median $\delta^{18}\text{O}$ value. The dots represent outliers that were outside the interquartile range. The number in the parentheses is the number of samples.

when atmospheric CO_2 concentrations were much lower than during interglacial times (Sigman and Boyle, 2000). However, it is likely that regional temperatures override this factor, with lower last glacial temperatures being more important than CO_2 in determining the relative abundance of C_3 and C_4 plants, as seen in Muhs et al. (1999).

C_4 plant occurrences are mainly found in mid-latitudes and tropical grasslands. Hence, a negative shift in shell $\delta^{13}\text{C}$ values is most likely explained by lower $\delta^{13}\text{C}$ values in the vegetation composition of C_3 plants today, compared with the late glacial. This may be caused by changes in the water-use efficiency in C_3 plants in slightly drier conditions during the late glacial compared with today (Policy et al., 1993). Water-use efficiency of plants refers to the amount of CO_2 uptake through photosynthesis

versus water loss to transpiration. Carbon isotope discrimination occurs during photosynthesis, when plants preferentially take up the lighter ^{12}C isotope (Hubrick et al., 1986). When water is more limited, a plant's ability to discriminate between carbon isotopes is reduced, leaving plants with higher ^{13}C concentrations and more positive $\delta^{13}\text{C}$ values at drier conditions (Hubrick et al., 1986).

Paleo-temperature and precipitation inferences

Shell $\delta^{18}\text{O}$ values were compared with the oxygen isotope values of two well-studied paleoclimate proxies: (1) Recent and Pleistocene seawater $\delta^{18}\text{O}$ and (2) Greenland ice core $\delta^{18}\text{O}$ values (Fig. 6). For seawater, we can evaluate time series of $\delta^{18}\text{O}$ values of

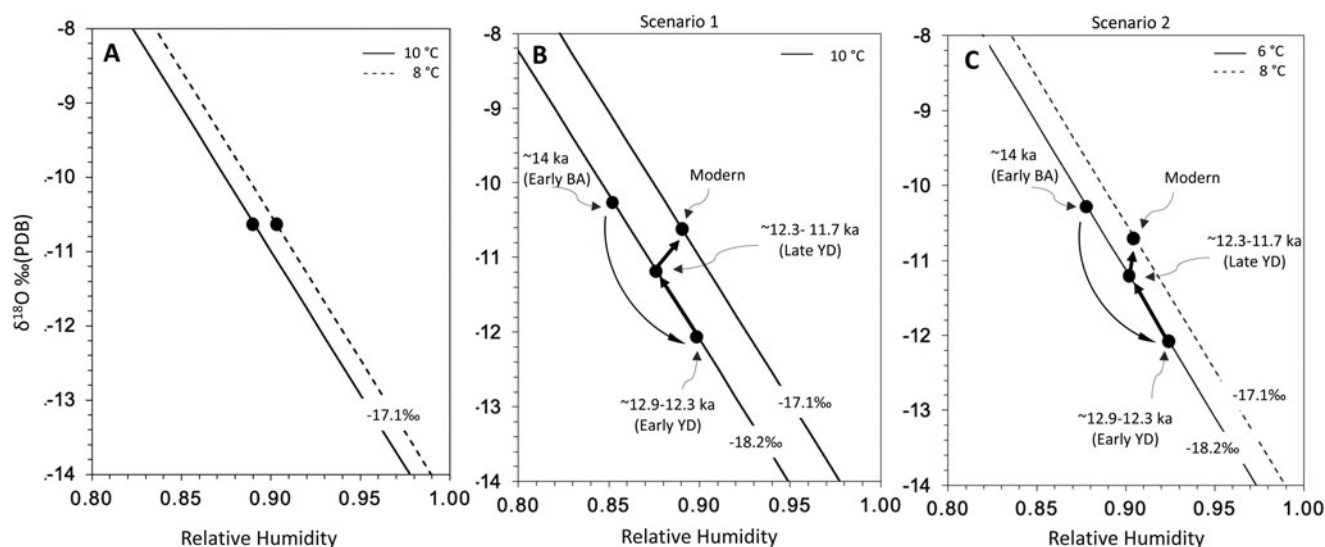


Figure 7. Calculated *Succinea* shell $\delta^{18}\text{O}$ values as a function of relative humidity (RH) using the evaporative steady-state flux balance mixing model by Balakrishnan and Yapp (2004). (A) Calculations for modern (live-collected) land snail shells from central Alaska assuming snails were active for an extended growing season, months of April to October (Nield et al., 2022). With rain $\delta^{18}\text{O}$ value of -17.1‰ SMOW, two possible temperature scenarios, 8°C (dashed line) and 10°C (solid line) (see text). Filled dots represent the average shell $\delta^{18}\text{O}$ value for modern shells. (B) Paleoclimatic scenario 1. Calculations were performed assuming snails were active only above 10°C (Cowie, 1984; Thompson, 1996) and rain $\delta^{18}\text{O}$ values (-18.2‰ SMOW) were estimated using the isotope–temperature coefficient at high latitudes (see text) (Rozanski et al., 1993). Filled dots represent the average shell $\delta^{18}\text{O}$ value for the early Bølling–Allerød (BA) (~ 14 ka), early Younger Dryas (YD), late YD, and modern. (C) Paleoclimate scenario 2. Calculations were performed using glacial temperature (6°C) estimated from a branched glycerol dialkyl glycerol tetraethers (brGDGT) record from a loess–paleosol sequence in interior Alaska (Kielhofer et al., 2023) and rain $\delta^{18}\text{O}$ value of -18.2‰ SMOW (Rozanski et al., 1993) (see text). Filled dots represent the average shell $\delta^{18}\text{O}$ value for the early BA (~ 14 ka) (-10.3‰), early YD (-12.1‰), late YD (-11.2‰), and modern (-10.7‰).

benthic foraminifera collected from the southwest coast of Alaska (Grebmeier et al., 1990; Fig. 1). Late-glacial seawater $\delta^{18}\text{O}$ averaged 1‰ , with low variability ($<1.5\text{‰}$). Modern seawater $\delta^{18}\text{O}$ off the coast of Alaska averages -1.1‰ , which is $\sim 2\text{‰}$ lower than late-glacial seawater $\delta^{18}\text{O}$ (Fig. 6A). Late-glacial $\delta^{18}\text{O}$ values were reported from the North Greenland Ice Core Project ice core (NGRIP Members, 2004) and modern $\delta^{18}\text{O}$ values were reported from the North Greenland Eemian Ice Drilling (NEEM) ice core (Masson-Delmotte et al., 2015). Greenland ice core $\delta^{18}\text{O}$ compositions vary through the late glacial, averaging -39‰ during the early Bølling–Allerød (~ 14 ka) and shifting to -40.4‰ during both the early Younger Dryas (12.9–12.3 ka) and the late Younger Dryas (12.3–11.7 ka). Modern Greenland ice core $\delta^{18}\text{O}$ values are the highest, averaging -32.4‰ (Fig. 6C).

When comparing snail shell $\delta^{18}\text{O}$ values with those of seawater and Greenland ice core records, it is important to recognize that they are recording different periods of time: seawater and ice core records generally average inputs across annual timescales (Grebmeier et al., 1990; Masson-Delmotte et al., 2015), while snail values record signatures of their growing seasons (Yanes et al., 2019). Despite the differences in temporal resolutions, comparing snail shell $\delta^{18}\text{O}$ values to these well-established paleoclimatic proxies provides context that aids in the interpretation of the respective roles of precipitation and temperature in determining fossil snail shell $\delta^{18}\text{O}$ values in interior Alaska. Fluctuations in snail shell $\delta^{18}\text{O}$ values do not mimic either Alaska seawater $\delta^{18}\text{O}$ or Greenland ice core $\delta^{18}\text{O}$ trends, as indicated by their nonsignificant Pearson correlation. Changes in shell $\delta^{18}\text{O}$ values through the late glacial likely tracked a combination of several atmospheric conditions, including precipitation and water vapor $\delta^{18}\text{O}$ composition, air temperature, and local RH (Balakrishnan and Yapp, 2004). Similar to this study, other temperature proxies from

interior Alaska show results inconsistent with Greenland ice core records. The brGDGT temperature records from interior Alaska do not indicate warmer temperatures during the Bølling–Allerød or consistently cooler temperatures during the Younger Dryas, in contrast to Greenland ice core records (Kielhofer et al., 2023).

Flux balance model

Measured shell $\delta^{18}\text{O}$ values from this study, along with local temperature and precipitation $\delta^{18}\text{O}$ estimates gathered from previously published data (Rozanski et al., 1993; Kielhofer et al., 2023), were used to apply the Balakrishnan and Yapp (2004) evaporative steady-state flux balance mixing model to estimate changes in late-glacial RH in interior Alaska. The model assumes (1) snail body water is lost through evaporation and (2) precipitation $\delta^{18}\text{O}$ and water vapor $\delta^{18}\text{O}$ values are in isotopic equilibrium. Despite the model's reliance on various unknown variables and assumptions, it can still provide a valuable nominal estimate of the RH at which snails grow. The flux balance model was used in this study to assess how RH changes from the early Bølling–Allerød to the early and late Younger Dryas with respect to the modern. Each period was analyzed under two temperature scenarios.

The model was applied to three late-glacial time periods: the early Bølling–Allerød (~ 14 ka), with an average shell $\delta^{18}\text{O}$ value of -10.3‰ ; the early Younger Dryas (12.9–12.3 ka), with an average shell $\delta^{18}\text{O}$ value of -12.1‰ ; and the late Younger Dryas (12.3–11.7 ka), with an average shell $\delta^{18}\text{O}$ value of -11.2‰ . Scenario 1 assumes snails were active only above 10°C (Cowie, 1984; Thompson, 1996). Precipitation $\delta^{18}\text{O}$ was calculated from the Rozanski et al. (1993) isotope–temperature

coefficient at high latitudes. These investigations reported that precipitation $\delta^{18}\text{O}$ decreases by 0.58‰ for every 1°C of temperature decrease. Therefore, if temperatures decreased by $\sim 2^\circ\text{C}$ during the last glacial period (Kielhofer et al., 2023) and modern rainwater $\delta^{18}\text{O}$ is -17.1‰ , paleontological rainwater $\delta^{18}\text{O}$ would have been -18.2‰ (Standard Mean Ocean Water [SMOW]) at this site. If this scenario is valid, then interior Alaska snails dating to the early Bølling–Allerød (~ 14 ka), with an average shell $\delta^{18}\text{O}$ value of -10.3‰ , grew at times when snails were active at 10°C , precipitation $\delta^{18}\text{O}$ was -18.2‰ , and RH was 85% (Fig. 7B). Shells dating to the early Younger Dryas (12.9–12.3 ka PB), with an average shell $\delta^{18}\text{O}$ value of -12.1‰ , grew at times when snails were active at 10°C , precipitation $\delta^{18}\text{O}$ was -18.2‰ , and RH was 90% (Fig. 7B). Shells dating to the late Younger Dryas (12.3–11.7 ka), with an average shell $\delta^{18}\text{O}$ value of -11.2‰ , grew at times when snails were active at 10°C , precipitation $\delta^{18}\text{O}$ was -18.2‰ , and RH was 87% (Fig. 7B).

Because snail activity has not been studied in detail in high-latitude regions, and some previous work has documented that snails track extended summer (April–October) atmospheric conditions (Nield et al., 2022), it is possible that *Succinea* snails could be active at temperatures below 10°C . Hence, scenario 2 assumes modern snails are active at 8°C . This scenario further assumes that late-glacial snails were active at 6°C , as inferred from a nearby brGDGT record, which found growing season temperatures during the Younger Dryas were approximately $\sim 2^\circ\text{C}$ colder than modern temperatures in interior Alaska, on average 8°C during the snail active period (Kielhofer et al., 2023). Precipitation $\delta^{18}\text{O}$ was estimated at -18.2‰ (SMOW), based on the Rozanski et al. (1993) equation, as calculated earlier. If this scenario is valid, then interior Alaska snails dating to the early Bølling–Allerød (~ 14 ka), with an average shell $\delta^{18}\text{O}$ value of -10.3‰ , grew at times when temperatures were 6°C , precipitation $\delta^{18}\text{O}$ was -18.2‰ , and RH was 88% (Fig. 7C). Shells dating to the early Younger Dryas (12.9–12.3 ka PB), with an average shell $\delta^{18}\text{O}$ value of -12.1‰ , grew at times when temperatures were 6°C , precipitation $\delta^{18}\text{O}$ was -18.2‰ , and RH was 92% (Fig. 7C). Shells dating to the late Younger Dryas (12.3–11.7 ka), with an average shell $\delta^{18}\text{O}$ value of -11.2‰ , grew at times when temperatures were 6°C , precipitation $\delta^{18}\text{O}$ was -18.2‰ , and RH was 90% (Fig. 7C).

Calculations using the flux balance model for modern (live-collected) land snails from interior Alaska were made assuming snails were active for an extended growing season, April–October, as suggested by prior work (Nield et al., 2022). A precipitation $\delta^{18}\text{O}$ value of -17.1‰ (SMOW) was assumed based on modeled results from IAEA/WMO (2015) by Bowen et al. (2005) (Fig. 7A). Model calculations were again performed at two possible temperature scenarios, 8°C , average extended growing season temperature in interior Alaska, and 10°C (Fig. 7A). If the assumptions behind these two scenarios are valid, then modern snails with an average shell $\delta^{18}\text{O}$ value of -10.7‰ , grew at times when RH was ~ 89 – 90% (Fig. 7A).

In both plausible situations, modern RH is predicted to be higher than in the early Bølling–Allerød, lower than in the early Younger Dryas, and similar to or slightly higher than in the late Younger Dryas (Fig. 7). Both scenarios predict high RH values ($>85\%$) at all time intervals studied. This interpretation is plausible, as snails are mainly active during or directly after rain events, when RH is the highest (Ward and Slotow, 1992).

Paleo-humidity fluctuations during the Younger Dryas

As inferred from the Balakrishnan and Yapp (2004) flux balance model, RH varied through the late-glacial period. In this study (14–11.5 ka), the lowest RH was found during the early Bølling–Allerød (~ 14 ka). Similar to previously discussed paleoclimate proxies (e.g., Bigelow and Edwards, 2001; Kielhofer et al., 2023), the data presented here do not show a dramatic climate shift at the start of the Younger Dryas. Shell $\delta^{18}\text{O}$ values from 13.5 to 12.8 ka have values similar to those of the early Younger Dryas, suggesting similar RH levels (Fig. 6A). Some paleoclimate studies in central and northern Alaska reported a prolonged dry period leading up to the Younger Dryas (Abbott et al., 2000; Edwards et al., 2001; Rabanus-Wallace et al., 2017), which we observed in the early Bølling–Allerød (~ 14 ka). This is likely due to a combination of factors, including the presence of the continental ice sheets, increased summer insolation, cool sea-surface temperatures, and lower sea levels during the late-glacial (Abbott et al., 2000). During the last glacial period, the Cordilleran and Laurentide Ice Sheets have been modeled as deflecting the westerlies south of their modern track, causing lower moisture in interior Alaska compared with today (COHMAP Members, 1988). Additionally, reduced North Atlantic Ocean sea-surface temperatures could have affected westerly flow and the strength of the Aleutian low air-pressure system (Kokorowski et al., 2008). Sea level was ~ 100 to 120 m lower than today, leaving portions of the Bering shelf exposed, increasing the distance for moisture transport to interior Alaska (Clark et al., 2014).

Our data suggest an increase in RH after the drier early Bølling–Allerød. RH through the Younger Dryas does not seem to be constant, as our data imply a two-stage climate pattern. The offset in snail shell oxygen isotope values between the early Younger Dryas (12.9–12.3 ka) and the late Younger Dryas (12.3–11.7 ka) is $\sim 1\text{‰}$. According to results from the flux balance model (Balakrishnan and Yapp 2004), this implies a wetter early Younger Dryas and subsequent drier late Younger Dryas. This two-step Younger Dryas phenomenon has been observed in other locations in Alaska (Kaufman et al., 2010) and globally (Brauer et al., 1999; Bakke et al., 2009; Scholaut et al., 2017; Pigati and Springer, 2022).

The Younger Dryas is well documented in southern and coastal Alaska (Kokorowski et al., 2008). In these regions, the results contradict the findings reported in this study, pointing to a mild early Younger Dryas and subsequently wetter late Younger Dryas. Jones et al. (2009) observed an increase in Polypodiaceae (fern) spores from a peat core in Swanson Fen (southwestern Alaska), indicating an increase in moisture around 12.2 ka. This agrees with paleoclimatic inferences from diatom assemblages at Arolik Lake (Hu et al., 2006), pollen records in nearby Nimgun Lake (Hu et al., 2002), and pollen and microfossil assemblages from Discovery Pond (Kaufman et al., 2010). However, all these sites are closer to coastal moisture sources compared with interior Alaska (this study).

Late-glacial paleoclimate records in interior Alaska, although not as abundant as those in southern Alaska, can be compared with our results. Abbott et al. (2000) studied lake-level history from seismic profiles and sediment cores of Birch Lake, located ~ 50 km from three of the archaeological sites analyzed in this study: Mead, Bachner, and North Gerstle. Lake systems in interior Alaska are sensitive to climate change and respond rapidly to moisture changes. In agreement with snail shell $\delta^{18}\text{O}$ values, the

Table 3. Institutional abbreviations and codes for snails collected from the Cold Regions Research and Engineering Laboratory (CRREL) permafrost tunnel.^a

Sample ID	Organism	Genera	locality	$\delta^{18}\text{O}$ (PDB)	$\delta^{13}\text{C}$ (PDB)	Catalog #/ Vial name
A02e	Snail	<i>Succinea</i>	Site A	-11.9	-7.5	UAM:ES:52634
A02g	Snail	<i>Succinea</i>	Site A	-8.3	-7.7	UAM:ES:52634
AOSb	Snail	<i>Succinea</i>	Site A	-12.2	-9.9	UAM:ES:52634
B09b	Snail	<i>Succinea</i>	Site B	-10.5	-9.5	UAM:ES:52632
B09h	Snail	<i>Succinea</i>	Site B	-9.1	-6.3	UAM:ES:52632
B09k	Snail	<i>Succinea</i>	Site B	-9	-5.9	UAM:ES:52632
B06c	Snail	<i>Succinea</i>	Site B	-10.6	-6	UAM:ES:52630
B06e	Snail	<i>Succinea</i>	Site B	-9.2	-6.6	UAM:ES:52630

^aUAM:ES, University of Alaska Museum of the North Earth Sciences Collection, Fairbanks.

lake levels at Birch Lake suggest there was an increase in humidity at the beginning of the Younger Dryas, with lake levels rising dramatically (by 18 m) between 12.7 and 12.2 ka and then stabilizing during the late Younger Dryas.

Today, the moisture in interior Alaska is mainly obtained from a westerly flow from the North Pacific Ocean and is related to large-scale atmospheric circulation patterns (Abbott et al., 2000; Kokorowski et al., 2008; Chipman et al., 2012). At the start of the Younger Dryas, interior Alaskan paleoclimate proxies suggest an increase in moisture. This change in RH could be caused by the change in sea level, which rose 30 m from 12.5 to 11.6 ka (Clark et al., 2014), or the decrease in size of the Cordilleran and Laurentide Ice Sheets, which affected circulation. As the ice sheets decreased, their impact on circulation would have diminished, making circulation patterns more like those of today (Bartlein et al., 1991).

CONCLUSIONS

The $\delta^{13}\text{C}$ values of *Succinea* shells in interior Alaska suggest that $\delta^{13}\text{C}$ values of late-glacial vegetation were consistently more positive than those of modern shells. Part of this difference is probably due to changes in the $\delta^{13}\text{C}$ value of CO_2 because of the increased burning of fossil fuels (Suess effect), which affects the $\delta^{13}\text{C}$ values of consumed plants. The rest of the offset is likely explained by changes in the $\delta^{13}\text{C}$ composition of C_3 plants consumed by snails. This is possibly explained by changes in the water-use efficiency of C_3 plants during the slightly drier late-glacial period compared with today, which would leave plants, and therefore snail shells, more enriched in ^{13}C due to changes in isotope discrimination during slightly drier conditions.

The $\delta^{18}\text{O}$ values of late-glacial *Succinea* shells in interior Alaska appear to record changes in RH over the late glacial. RH was modeled using the Balakrishnan and Yapp (2004) flux balance mixing model. The results show RH increased from ~14 ka to the early Younger Dryas (~12.9–12.3 ka), then decreased in the latter half of the Younger Dryas (~12.3–11.7 ka), with modern conditions being similar to those in the late Younger Dryas. Shell $\delta^{18}\text{O}$ values from interior Alaska highlight a two-stage humidity pattern during the Younger Dryas, which other studies have found evidence of at other sites in interior Alaska and elsewhere in North America. Published climate and humidity records in Alaska during the Younger Dryas are somewhat complex; however, lake proxies from interior Alaska agree with our

findings and show evidence for a wetter early Younger Dryas compared with other periods of the late glacial.

This study illustrates that ancient land snails may be useful for clarifying the complex climatic history of the late glacial in interior Alaska. Isotope records dating to the late glacial in interior Alaska are rare. Additional isotope records dating to the Younger Dryas may help solidify emerging patterns about late-glacial humidity in interior Alaska.

Acknowledgments. This project was funded by National Science Foundation grants EAR-1529133 and 1802153 to YY. Additional funding was awarded to CBN from the Geological Society of America (GSA), Paleontological Society, Western Interior Paleontological Society (WIPS), Society for Sedimentary Geology (SEPM), and Sigma Xi (Scientific Research Society). Special thanks go to Jason Curtis (University of Florida) for assistance with isotope analyses; John Southon (University of California–Irvine) for assistance with radiocarbon analyses; Ezekiel King Phillips for field assistance collecting modern and fossil samples; Julie Esdale for archaeological site field assistance; Briana Doering (University of Wyoming) for samples from Bachner; Ben Potter, Gerad Smith, Chuck Holmes, and Barbara Crass (University of Alaska Fairbanks) for support in sampling Upward Sun River site and Mead and North Gerstle sites; George Harrison, William Wright, John Scot, and Thomas Sniezak for sampling shells from the permafrost tunnel; the U.S. Army Corps of Engineers, CRREL and Gary Larsen for tunnel access; and the U.S. Army for land access. Funding for JSP and DRM was provided by the U.S. Geological Survey's Climate and Land Use Change Research and Development Program through the Quaternary Hydroclimate Records of Spring Ecosystems project. Any use of trade, firm, or product names is for descriptive purposes only and does not imply endorsement by the U.S. government.

Data Availability Statement. Downloadable files of the data presented in Tables 1–3 can be found at <https://doi.org/10.5066/P953H59T>.

REFERENCES

- Abbott, M.B., Finney, B.P., Edwards, M.E., Kelts, K.R., 2000. Ltanane-level reconstruction and paleohydrology of Birch Lake, central Alaska, based on seismic reflection profiles and core transects. *Quaternary Research* 53, 154–166.
- Alley, R.B., Meese, D.A., Shuman, C.A., Gow, A.J., Taylor, K.C., Grootes, P.M., White, J.W.C., et al., 1993. Abrupt increase in Greenland snow accumulation at the end of the Younger Dryas event. *Nature* 362, 527–529.
- Anderson, P.M., 2003. The Quaternary period in the United States results and paleoclimate implications of 35 years of paleoecological research in Alaska. *Quaternary Sciences* 1, 427–440.
- Bakke, J., Heegaard, E., Haug, G.H., Birks, H.H., Nilsen, T., Lie, Ø, Dulski, P., Dokken, T., 2009. Rapid oceanic and atmospheric changes during the Younger Dryas cold period: *Nature Geoscience* 2, 202–205.

- Balakrishnan, M., Yapp, C.J.**, 2004. Flux balance models for the oxygen and carbon isotope compositions of land snail shells. *Geochimica et Cosmochimica Acta* **68**, 2007–2024.
- Bartlein, P.J., Anderson, P.M., Edwards, M.E., Mcdowell, P.F.**, 1991. A framework for interpreting paleoclimatic variations in Eastern Beringia. *Quaternary International* 10–12, 73.
- Bigelow, N.H., Edwards, M.E.**, 2001. A 14,000yr paleoenvironmental record from Windmill Lake, central Alaska: late glacial and Holocene vegetation in the Alaska range. *Quaternary Science Reviews* **20**, 203.
- Bigelow, N.H., Powers, W.R.**, 2001. Climate, vegetation, and archaeology 14,000–9000 cal yr B.P. in central Alaska. *Arctic Anthropology* **38**, 171–195.
- Boers, N.**, 2021. Observation-based early-warning signals for a collapse of the Atlantic Meridional Overturning Circulation. *Nature Climate Change* **11**, 680–688.
- Bowen, G.J.**, 2020. Gridded Maps of the Isotopic Composition of Meteoric Waters. <http://www.waterisotopes.org>.
- Bowen, G.J., Wassenaar, L.I., Hobson, K.A.**, 2005. Global application of stable hydrogen and oxygen isotopes to wildlife forensics. *Oecologia* **143**, 337–348.
- Brauer, A., Endres, C., Günter, C., Litt, T., Stebich, M., Negendank, J.F.W.**, 1999. High resolution sediment and vegetation responses to Younger Dryas climate change in varved lake sediments from Meerfelder Maar, Germany. *Quaternary Science Reviews* **18**, 321.
- Bright, J., Ebert, C., Kosnik, M.A., Southon, J.R., Whitacre, K., Albano, P.G., Flores, C., et al.**, 2021. Comparing direct carbonate and standard graphite ^{14}C determinations of biogenic carbonates. *Radiocarbon* **63**, 387–403.
- Broecker, W.S., Denton, G.H., Edwards, R.L., Cheng, H., Alley, R.B., Putnam, A.E.**, 2010. Putting the Younger Dryas cold event into context. *Quaternary Science Reviews* **29**, 1078–1081.
- Chipman, M.L., Clegg, B.F., Hu, F.S.**, 2012. Variation in the moisture regime of northeastern interior Alaska and possible linkages to the Aleutian Low: inferences from a late-Holocene $\delta^{18}\text{O}$ record. *Journal of Paleolimnology* **48**, 69–81.
- Clark, J., Mitrovica, J.X., Alder, J.**, 2014. Coastal paleogeography of the California–Oregon–Washington and Bering Sea continental shelves during the latest Pleistocene and Holocene: implications for the archaeological record. *Journal of Archaeological Science* **52**, 12–23.
- COHMAP Members**, 1988. Climatic changes of the last 18,000 years: observations and model simulations. *Science* **241**, 1043–1052.
- Cowie, R.H.**, 1984. The life-cycle and productivity of the land snail *Theba pisana* (Mollusca: Helicidae). *Journal of Animal Ecology* **53**, 311–325.
- Dawson, T.E., Mambelli, S., Plamboeck, A.H., Templer, P.H., Tu, K.P.**, 2002. Stable isotopes in plant ecology. *Annual Review of Ecology and Systematics* **33**, 507–559.
- Dilley, T.E.**, 1998. Late Quaternary Loess Stratigraphy, Soils, and Environments of the Shaw Creek Flats Paleoindian Sites, Tanana Valley, Alaska. PhD thesis, University of Tucson, Tucson.
- Edwards, M.E., Mock, C.J., Finney, B.P., Barber, V.A., Bartlein, P.J.**, 2001. Potential analogues for paleoclimatic variations in eastern interior Alaska during the past 14,000yr: atmospheric-circulation controls of regional temperature and moisture responses. *Quaternary Science Reviews* **20**, 189.
- Friedli, H., Loetscher, H., Oeschger, H., Siegenthaler, U., Stauffer, B.**, 1986. Ice core record of the C-13/C-12 ratio of atmospheric CO_2 in the past two centuries. *Nature* **324**, 237.
- Goodfriend, G.A.**, 1990. Rainfall in the Negev Desert during the middle Holocene, based on ^{13}C of organic matter in land snail shells. *Quaternary Research* **34**, 186–197.
- Goodfriend, G.A.**, 1991. Holocene trends in ^{18}O in land snail shells from the Negev Desert and their implications for changes in rainfall source areas. *Quaternary Research* **35**, 417–426.
- Goodfriend, G.A.**, 1992. The use of land snail shells in paleoenvironmental reconstruction. *Quaternary Science Reviews* **11**, 665–685.
- Goodfriend, G.A., Ellis, G.L.**, 2000. Stable carbon isotope record of middle to late Holocene climate changes from land snail shells at Hinds Cave, Texas. *Quaternary International* **67**, 47–60.
- Goodfriend, G.A., Ellis, G.L.**, 2002. Stable carbon and oxygen isotopic variations in modern *Rabdotus* land snail shells in the southern Great Plains, USA, and their relation to environment. *Geochimica et Cosmochimica Acta* **66**, 1987–2002.
- Goodfriend, G.A., Hood, D.G.**, 1983. Carbon isotope analysis of land snail shells: implications for carbon sources and radiocarbon dating. *Radiocarbon* **25**, 810–830.
- Goodfriend, G.A., Stipp, J.J.**, 1983. Limestone and the problem of radiocarbon dating of land-snail shell carbonate. *Geology* **11**, 575–577.
- Graf, K.E., Bigelow, N.H.**, 2011. Human response to climate during the Younger Dryas chronozone in central Alaska. *Quaternary International* **242**, 434–451.
- Grebmeier, J.M., Cooper, L.W., DeNiro, M.J.**, 1990. Oxygen isotopic composition of bottom seawater and tunicate cellulose used as indicators of water masses in the northern Bering and Chukchi Seas. *Limnology and Oceanography* **35**, 1182–1195.
- Hamilton, T.D., Craig, J.L., Sellmann, P.V.**, 1988. The Fox permafrost tunnel: a late Quaternary geologic record in central Alaska, with Suppl. Data 88-11. *Geological Society of America Bulletin* **100**, 948–969.
- Hubick, K.T., Farquhar, G.D., Shorter, R.**, 1986. Correlation between water-use efficiency and carbon isotope discrimination in diverse peanut (*Arachis*) germplasm. *Australian Journal of Plant Physiology* **13**, 803–816.
- Hu, F.S., Lee, B.Y., Kaufman, D.S., Yoneji, S., Nelson, D.M., Henne, P.D.**, 2002. Response of tundra ecosystem in southwestern Alaska to Younger-Dryas climatic oscillation. *Global Change Biology* **8**, 1156–1163.
- Hu, F.S., Nelson, D.M., Clarke, G.H., Rühland, K.M., Huang, Y., Kaufman, D.S., Smol, J.P.**, 2006. Abrupt climatic events during the last glacial-interglacial transition in Alaska. *Geophysical Research Letters* **33**, L18708-n/a.
- Hu, F.S., Shemesh, A.**, 2003. A biogenic-silica $\delta^{18}\text{O}$ record of climatic change during the last glacial–interglacial transition in southwestern Alaska. *Quaternary Research* **59**, 379.
- [IAEA/WMO] International Atomic Energy Agency/World Meteorological Organization**, 2015. Global network of isotopes in precipitation. NGIP Database. doi: <https://nucleus.iaea.org/>.
- Jones, M.C., Peteet, D.M., Kurdyla, D., Guilderson, T.**, 2009. Climate and vegetation history from a 14,000-year peatland record, Kenai Peninsula, Alaska. *Quaternary Research* **72**, 207–217.
- Kanevskiy, M., Shur, Y., Bigelow, N.H., Bjella, K.L., Douglas, T.A., Fortier, D., Jones, B.M., Jorgenson, M.T.**, 2022. Yedoma cryostratigraphy of recently excavated sections of the CRREL permafrost tunnel near Fairbanks, Alaska. *Frontiers in Earth Science* **9**, doi: 10.3389/feart.2021.758800.
- Kaufman, D.S., Axford, Y., Anderson, R.S., Lamoureux, S.F., Schindler, D.E., Walker, I.R., Werner, A.**, 2012. multi-proxy record of the Last Glacial Maximum and last 14,500 years of paleoenvironmental change at Lone Spruce Pond, southwestern Alaska. *Journal of Paleolimnology* **48**, 9–26.
- Kaufman, D.S., Schneider, D.P., McKay, N.P., Ammann, C.M., Bradley, R.S., Briffa, K.R., Miller, G.H., Otto-Bliesner, B.L., Overpeck, J.T., Vinther, B.M.**, 2009. Recent warming reverses long-term arctic cooling. *Science* **325**, 1236.
- Kaufman, D.S., Scott Anderson, R., Hu, F.S., Berg, E., Werner, A.**, 2010. Evidence for a variable and wet Younger Dryas in southern Alaska. *Quaternary Science Reviews* **29**, 1445–1452.
- Keeling, C.D.**, 1979. The Suess effect: ^{13}C -carbon- ^{14}C carbon interrelations. *Environment International* **2**, 229.
- Kielhofer, J.R., Miller, C.C., Reuther, J., Holmes, C., Potter, B., Lanoë, F., Esdale, J., Crass, B.**, 2020. The micromorphology of loess-paleosol sequences in central Alaska: a new perspective on soil formation and landscape evolution since the Late Glacial period (c. 16,000 cal yr BP to present). *Geoarchaeology* **35**, 701.
- Kielhofer, J.R., Tierney, J.E., Reuther, J.D., Potter, B.A., Holmes, C.E., Lanoë, F.B., Esdale, J.A., Wooller, M.J., Bigelow, N.H.**, 2023. BrGDGT temperature reconstruction from interior Alaska: assessing 14,000 years of deglacial to Holocene temperature variability and potential effects on early human settlement. *Quaternary Science Reviews* **303**, 107979.
- Kokorowski, H.D., Anderson, P.M., Mock, C.J., Lozhkin, A.V.**, 2008. A re-evaluation and spatial analysis of evidence for a Younger Dryas climatic reversal in Beringia. *Quaternary Science Reviews* **27**, 1710–1722.

- Kurek, J., Cwynar, L.C., Ager, T.A., Abbott, M.B., Edwards, M.E., 2009. Late Quaternary paleoclimate of western Alaska inferred from fossil chironomids and its relation to vegetation histories. *Quaternary Science Reviews* **28**, 799–811.
- Lécolle, P., 1985. The oxygen isotope composition of land snail shells as a climatic indicator: applications to hydrogeology and paleoclimatology. *Chemical Geology: Isotope Geoscience Section* **58**, 157–181.
- Masson-Delmotte, V., Steen-Larsen, H.C., Ortega, P., Swingedouw, D., Popp, T., Vinther, B.M., Oerter, H., et al., 2015. Recent changes in north-west Greenland climate documented by NEM shallow ice core data and simulations, and implications for past-temperature reconstructions. *The Cryosphere* **9**, 1481–1504.
- Metref, S., Rousseau, D., Bentaleb, I., Labonne, M., Vianey-Liaud, M., 2003. Study of the diet effect on $\delta^{13}\text{C}$ of shell carbonate of the land snail *Helix aspersa* in experimental conditions. *Earth and Planetary Science Letters* **211**, 381.
- Moine, O., Rousseau, D., Antoine, P., 2005. Terrestrial molluscan records of Weichselian lower to middle pleniglacial climatic changes from the Nussloch loess series (Rhine Valley, Germany): the impact of local factors. *Boreas* **34**, 363–380.
- Muhs, D.R., Ager, T.A., Been, J.M., Rosenbaum, J.G., Reynolds, R.J., 2000. *An evaluation of methods for identifying and interpreting paleosols in late Quaternary loess in Alaska*. U.S. Geological Survey, Reston, VA, pp. 127–146.
- Muhs, D.R., Aleinikoff, J.N., Stafford, T.W., Jr., Kihl, R., Been, J., Mahan, S.A., Cowherd, S., 1999. Late Quaternary loess in northeastern Colorado: part I—age and paleoclimatic significance. *Geological Society of America Bulletin* **111**, 1861–1875.
- Muhs, D.R., Pigati, J.S., Budahn, J.R., Skipp, G.L., Bettis, E.A., Jensen, B., 2018. Origin of last-glacial loess in the western Yukon-Tanana Upland, central Alaska, USA. *Quaternary Research* **89**, 797–819.
- Nekola, J., 2014. Overview of the North American terrestrial gastropod Fauna. *American Malacological Bulletin* **32**, 225–235.
- Nield, C.B., Yanes, Y., Pigati, J.S., Rech, J.A., von Proschwitz, T., Nekola, J.C., 2022. Oxygen isotopes of land snail shells in high latitude regions. *Quaternary Science Reviews* **279**, 107382.
- North Greenland Ice Core Project Members, 2004. High resolution record of Northern Hemisphere climate extending into the last interglacial period. *Nature* **431**, 147.
- Oerstan, A., 2010. Reproductive biology and annual population cycle of *Oxyloma retusum* (Pulmonata: Succineidae). *American Malacological Bulletin* **28**, 113–120.
- O'Leary, M.H., 1988. Carbon isotopes in photosynthesis. *BioScience* **38**, 328–336.
- Pewe, T.L., 1975. Quaternary Geology of Alaska. U.S. Geological Survey Professional Paper **835**.
- Pigati, J.S., McGeehin, J.P., Muhs, D.R., Bettis, E.A., 2013. Radiocarbon dating late Quaternary loess deposits using small terrestrial gastropod shells. *Quaternary Science Reviews* **76**, 114–128.
- Pigati, J.S., Quade, J., Shahanan, T.M., Haynes, C.V., 2004. Radiocarbon dating of minute gastropods and new constraints on the timing of late Quaternary spring-discharge deposits in southern Arizona, USA. *Palaeogeography, Palaeoclimatology, Palaeoecology* **204**, 33.
- Pigati, J.S., Rech, J.A., Nekola, J.C., 2010. Radiocarbon dating of small terrestrial gastropod shells in North America. *Quaternary Geochronology* **5**, 519–532.
- Pigati, J.S., Springer, K.B., 2022. Hydroclimate response of spring ecosystems to a two-stage Younger Dryas event in western North America. *Scientific Reports* **12**, 7323.
- Policy, H.W., Johnson, H.B., Marino, B.D., Mayeux, H.S., 1993. Increase in C_3 plant water-use efficiency and biomass over Glacial to present CO_2 concentrations. *Nature* **361**, 61–64.
- Potter, B.A., Holmes, C.E., Yesner, D.R., 2013. Technology and economy among the earliest prehistoric foragers in interior eastern Beringia. In: Graf, K.E., Ketron, C.V., Waters, M.R. (Eds.), *Paleoamerican Odyssey*. Texas A&M University Press, College Station, pp. 81–103.
- Potter, B.A., Irish, J.D., Reuther, J.D., Gelvin-Reymiller, C., Holliday, V.T., 2011. A Terminal Pleistocene child cremation and residential structure from eastern Beringia. *Science* **331**, 1058–1062.
- Potter, B.A., Irish, J.D., Reuther, J.D., McKinney, H.J., 2014. New insights into Eastern Beringian mortuary behavior: a terminal Pleistocene double infant burial at Upward Sun River. *Proceedings of the National Academy of Sciences USA* **111**, 17060–17065.
- Praetorius, S.K., Mix, A.C., Walczak, M.H., Wolhowe, M.D., Addison, J.A., Prah, F.G., 2015. North Pacific deglacial hypoxic events linked to abrupt ocean warming. *Nature* **527**, 362–366.
- Praetorius, S., Mix, A., Jensen, B., Froese, D., Milne, G., Wolhowe, M., Addison, J., Prah, F., 2016. Interaction between climate, volcanism, and isostatic rebound in southeast Alaska during the last deglaciation. *Earth and Planetary Science Letters* **452**, 79–89.
- Rabanus-Wallace, M.T., Wooller, M.J., Zazula, G.D., Shute, E., Jahren, A.H., Kosintsev, P., Burns, J.A., Breen, J., Llamas, B., Cooper, A., 2017. Megafaunal isotopes reveal role of increased moisture on rangeland during late Pleistocene extinctions. *Nature Ecology and Evolution* **1**, 0125.
- R Core Team, 2023. *R: A Language and Environment for Statistical Computing*. R Foundation for Statistical Computing, Vienna.
- Reimer, P.J., Austin, W.E.N., Bard, E., Bayliss, A., Blackwell, P.G., Bronk Ramsey, C., Butzin, M., et al., 2020. The IntCal20 Northern hemisphere radiocarbon age calibration curve (0–55 cal kBP). *Radiocarbon* **62**, 725–757.
- Reuther, J.D., 2013. Late Glacial and Early Holocene Geoarchaeology and Terrestrial Paleocology in the Lowlands of the Middle Tanana Valley, Subarctic Alaska. PhD thesis, University of Arizona, Tucson, Arizona.
- Riddle, W.A., 1983. Physiological ecology of land snails and slugs. In: Russell-Hunter, W.D. (Ed.), *Ecology*. Academic Press, Orlando, FL, pp. 431–461.
- Rozanski, K., Araguás-Araguás, L., Gonfiantini, R., 1993. Isotopic patterns in modern global precipitation, in climate change in continental isotopic records: Washington, D. C. *Climate Change in Continental Isotopic Records* **78**, 1–36.
- Rubinson, M., Clayton, R.N., 1969. Carbon-13 fractionation between aragonite and calcite. *Geochimica et Cosmochimica Acta* **33**, 997–1002.
- Schlolaut, G., Brauer, A., Nakagawa, T., Lamb, H.F., Tyler, J.J., Staff, R.A., Marshall, M.H., Bronk Ramsey, C., Bryant, C.L., Tarasov, P.E., 2017. Evidence for a bi-partition of the Younger Dryas Stadial in East Asia associated with inverted climate characteristics compared to Europe. *Scientific Reports* **7**, 44983.
- Seierstad, I.K., Abbott, P.M., Bigler, M., Blunier, T., Bourne, A.J., Brook, E., Buchardt, S.L., et al., 2014. Consistently dated records from the Greenland GRIP, GISP2 and NGRIP ice cores for the past 104 ka reveal regional millennial-scale $\delta^{18}\text{O}$ gradients with possible Heinrich event imprint. *Quaternary Science Reviews* **106**, 29–46.
- Shur, Y., French, H.M., Bray, M.T., Anderson, D.A., 2004. Syngenetic permafrost growth: cryostratigraphic observations from the CRREL tunnel near Fairbanks, Alaska. *Permafrost and Periglacial Processes* **15**, 339–347.
- Sigman, D.M., Boyle, E.A., 2000. Glacial/interglacial variations in atmospheric carbon dioxide. *Nature* **407**, 859–869.
- Stewart, B.C., Kunkel, K.E., Stevens, L.E., Sun, L., Walsh, J.E., 2013. Regional Climate Trends and Scenarios for the US National Climate Assessment: Part 7. Climate of Alaska. NOAA Technical Report NESDIS **142**(7).
- Stott, L.D., 2002. The influence of diet on the $\delta^{13}\text{C}$ of shell carbon in the pulmonate snail *Helix aspersa*. *Earth and Planetary Science Letters* **195**, 249.
- Taylor, P.C., Maslowski, W., Perlwitz, J., Wuebbles, D.J., 2017. *Climate Science Special Report: Fourth National Climate Assessment*. Vol. I. doi: <https://doi.org/10.7930/J00863GK>.
- Thompson, R., 1996. *Raising Snails*. U.S. Department of Agriculture, National Agricultural Library, Beltsville, MD.
- Vanderhoek, R., Dilley, T., Holmes, C., 1997. North Gerstle Point: a deeply stratified multi-component site in the central Tanana Valley, Alaska. Paper Presented at the 1997 Alaska Anthropology Association Meeting, Whitehorse, Yukon.
- Viereck, L.A., Little, E.L., 1994. *Alaska Trees and Shrubs*. University of Alaska Press, Fairbanks.
- Walker, M., Johnsen, S., Rasmussen, S.O., Popp, T., Steffensen, J., Gibbard, P., Hoek, W., et al., 2009. Formal definition and dating of the GSSP (Global Stratotype Section and Point) for the base of the Holocene using the Greenland NGRIP ice core, and selected auxiliary records. *Journal of Quaternary Science* **24**, 3–17.

- Walsh, J.E., Brettschneider, B., 2019. Attribution of recent warming in Alaska. *Polar Science* **21**, 101–109.
- Wang, F., Gao, J., Yong, J.W.H., Wang, Q., Ma, J., He, X., 2020. Higher atmospheric CO₂ levels favor C₃ plants over C₄ plants in utilizing ammonium as a nitrogen source. *Frontiers in Plant Science* **11**, 537443.
- Wang, T., Surge, D., Walker, K.J., 2011. Isotopic evidence for climate change during the Vandal Minimum from *Ariopsis felis* otoliths and *Mercenaria campechiensis* shells, southwest Florida, USA. *The Holocene* **21**, 1081–1091.
- Ward, D., Slotow, R., 1992. The effects of water availability on the life history of the desert snail, *Trochoidea seetzeni*. An experimental field manipulation. *Oecologia* **90**, 572–580.
- Wooller, M.J., Zazula, G.D., Edwards, M., Froese, D.G., Boone, R.D., Parker, C., Bennett, B., 2018. Stable carbon isotope compositions of eastern Beringian grasses and sedges: investigating their potential as paleoenvironmental indicators. *Arctic, Antarctic, and Alpine Research* **39**, 318.
- Yanes, Y., Al-Qattan, N.M., Rech, J.A., Pigati, J.S., Dodd, J.P., Nekola, J.C., 2019. Overview of the oxygen isotope systematics of land snails from North America. *Quaternary Research* **91**, 329–344.
- Yanes, Y., Delgado, A., Castillo, C., Alonso, M.R., Ibáñez, M., De la Nuez, J., Kowalewski, M., 2008. Stable isotope ($\delta^{18}\text{O}$, $\delta^{13}\text{C}$, and δD) signatures of recent terrestrial communities from a low-latitude, oceanic setting: endemic land snails, plants, rain, and carbonate sediments from the eastern Canary Islands. *Chemical Geology* **249**, 377–392.
- Yanes, Y., Nekola, J.C., Rech, J.A., Pigati, J.S., 2017. Oxygen stable isotopic disparities among sympatric small land snail species from northwest Minnesota, USA. *Palaeogeography, Palaeoclimatology, Palaeoecology* **485**, 715–722.
- Yanes, Y., Romanek, C.S., Delgado, A., Brant, H.A., Noakes, J.E., Alonso, M.R., Ibáñez, M., 2009. Oxygen and carbon stable isotopes of modern land snail shells as environmental indicators from a low-latitude oceanic island. *Geochimica et Cosmochimica Acta* **73**, 4077–4099.
- Yanes, Y., Yapp, C.J., Ibáñez, M., Alonso, M.R., De-la-Nuez, J., Quesada, M.L., Castillo, C., Delgado, A., 2011. Pleistocene–Holocene environmental change in the Canary Archipelago as inferred from the stable isotope composition of land snail shells. *Quaternary Research* **75**, 658–669.
- Zanchetta, G., Leone, G., Fallick, A.E., Bonadonna, F.P., 2005. Oxygen isotope composition of living land snail shells: data from Italy. *Palaeogeography, Palaeoclimatology, Palaeoecology* **223**, 20–33.
- Zhang, N., Yamada, K., Yoshida, N., 2018. Food water contribution to the oxygen isotope composition of land snail body water and its environmental implication. *Geochemistry, Geophysics, Geosystems* **19**, 1800.